Department of Chemistry
Faculty of Science
University of Helsinki
Finland

HYDROGEN AND WATER SPLITTING BY FRUSTRATED LEWIS PAIRS AND REACTIONS THEREOF

Kristina Sorochkina

DOCTORAL DISSERTATION

To be presented for public examination with the permission of the Faculty of Science of the University of Helsinki, in auditorium A111, Exactum (Pietari Kalmin katu 5, Helsinki), on the 25th of February 2022 at 12 o'clock.

Helsinki 2022

Supervisors

Professor Dr. Timo Repo
Department of Chemistry
University of Helsinki
Helsinki, Finland

Dr. Konstantin Chernichenko
API Small Molecule Development
Janssen Pharmaceutica N. V.
Beerse, Belgium

Reviewers

Associate Professor Dr. Daniela Bezuidenhout
Faculty of Technology
University of Oulu
Oulu, Finland

Dr. Tibor Soós
Institute of Organic Chemistry
Research Centre for Natural Sciences
Budapest, Hungary

Opponent

Professor Dr. Simon Aldridge
Department of Chemistry
University of Oxford
Oxford, United Kingdom

The Faculty of Science uses the Ouriginal system (plagiarism recognition) to examine all doctoral dissertations.

ISBN 978-951-51-7906-7 (paperback)
ISBN 978-951-51-7907-4 (PDF)

http://ethesis.helsinki.fi

Unigrafia
Helsinki 2022

ABSTRACT

The principle of combining a Lewis acid (LA) and a Lewis base (LB), prevented from the formation of classical Lewis adduct and thus possessing reactive potential, is known as frustrated Lewis pair (FLP). This powerful, yet simple concept allowed for a wide range of reactivities unprecedented for main group chemistry and is perceived as an alternative to transition metal catalysis. Among such reactivities, hydrogen activation and catalytic hydrogenations of unsaturated organic substrates, perhaps remain the most remarkable ones.

In the literature review, our focus is limited to hydrogen activation and reactions thereof, and furthermore, FLPs comprising boron-centered LAs. First, mechanistic aspects of the process are discussed, including principles of assessment and modulation of Lewis acidity. Further, the review covers hydrogenation catalysis with FLPs, including hydrogenation of polar and non-polar substrates, functional group- and moisture- tolerant catalysts, and enantioselective hydrogenations. A separate section is devoted to intramolecular FLPs as a distinct subclass of FLPs.

The results and discussion part summarizes the key findings reported in the attached original publications and can be divided into two subtopics. First is devoted to the development of linked FLPs aimed for generation of parahydrogen-induced hyperpolarization (PHIP). The phenomenon occurs upon parahydrogen (p-H_2) pairwise splitting and causes substantial amplification of NMR signals of p-H_2 originating fragments and neighboring nuclei. Therefore, the method can be promising for sensitivity enhancement in, e.g., NMR (MRI) signal imaging. In this work, the series of phenylene bridged *ansa*-aminoboranes (AABs) varied in the chemical environment around B were synthesised, and their ability to generate PHIP upon addition of p-H_2 at ambient conditions was demonstrated. Kinetic, thermodynamic, and NMR parameters favorable for the efficient production of PHIP with such FLPs were formulated. Replacement of quadrupolar ^{14}N nucleus of the amine site with ^{15}N in the series led to spontaneous polarization transfer to nitrogen and strong signal enhancements. Further efforts were dedicated to overcoming the incompatibility of ansa-FLPs with water, bringing closer their realization as PHIP contrast agents in biologically relevant media. In this regard, thorough design of LA-LB active sites resulted in *ansa*-phosphinoborane capable of both H_2 and H_2O splitting in a reversible manner. Quite unexpectedly, this compound featured stoichiometric reduction of H_2O to H_2 via a proton “umpolung” mechanism.

The second part is devoted to synthesizing (+)-camphor-based chiral boranes for asymmetric hydrogenation of imines. This study resulted in a highly enantioselective catalyst easily accessible from the synthetic point of view and shed light on the origin of the enantioselectivity.

ACKNOWLEDGEMENTS

This work was performed in 2016-2020 in the Division of Synthesis and Catalysis, Department of Chemistry, University of Helsinki. It was funded by Academy of Finland (projects 276586 and 316207) and by the Doctoral Program in Chemistry and Molecular Catalysis (CHEM), which are gratefully acknowledged.

I would like to express my deepest gratitude to my supervisor Prof. Timo Repo for giving me an opportunity to accomplish this study, for providing all the necessary conditions and resources for the research. I was fortunate to have such a supportive and experienced supervisor. I am deeply indebted to my co-supervisor Konstantin Chernichenko, who taught me experimental chemistry, and, more importantly, a scientific way of thinking which is now deeply rooted in my personality. He generously shared his knowledge, experience, and ideas, and certainly became one of the most influential persons I have met so far.

I would like to thank my collaborator Assoc. Prof. Vladimir Zhivonitko, without whom this work would not be possible. His dedication and passion for NMR and hyperpolarization techniques sparked my interest to work in this direction. I am grateful to Prof. Imre Pápai and Dr. Andea Hamza for fruitful collaboration on theoretical aspects of the work and their warm hospitality during my visit to Institute of Organic Chemistry in Budapest.

The help of personnel and teaching staff of the department cannot be overestimated. I am grateful to Dr. Martin Nieger for X-ray diffraction measurements, Dr. Sami Heikkinen for extensive assistance with NMR spectroscopy, and to Mikko Heikelä and Karina Moslova for helping with various technical and administrative issues. I appreciate the help of Hassan Haddad and Sami Virtanen with laboratory supplies.

I want to thank Dr. Jesus Perea-Buceta, Sarah Seefried, Aleksi Sahari, Jere Mannisto, Emi Lagerspets, Eeva Heliovara, Dr. Luc Chaboneau, Aleksi Eronen, Tom Wirtanen, Dr. Aleksandar Todorov, and all coworkers in Synthesis and Analysis research unit for creating a friendly environment, and leisure time we spent together.

I would like to thank my lifelong friends Kristina Goncharenko, Lubov Grineva and Yulianna Morozova, who always supported me in my endeavors.

I want to express my deepest gratitude to my mother Irina and my stepfather Yurii for the love, support, and resources they bestowed me so that I could grow personally and professionally.

I express special gratitude to my husband Nikos, whose love, unlimited patience, and optimism helped me to carry this work through, and to my daughter Katerina for lighting up my way.

CONTENTS

LIST OF ORIGINAL PUBLICATIONS

This thesis is based on the following publications:

I Vladimir Zhivonitko, **Kristina Sorochkina**, Konstantin Chernichenko, Bianka Kótai, Tamás Földes, Imre Pápai, Ville-Veikko Telkki, Timo Repo, and Igor Koptyug. Nuclear spin hyperpolarization with *ansa*-aminoboranes: a metal-free perspective for parahydrogen-induced polarization. *Phys. Chem. Chem. Phys.* **2016**, *18*, 27784-27795

II Konstantin Chernichenko, Markus Lindqvist, Bianka Kótai, Martin Nieger, **Kristina Sorochkina**, Imre Pápai, and T. Repo. Metal-Free sp^2-C–H Borylation as a common reactivity pattern of frustrated 2-aminophenylboranes. *J. Am. Chem. Soc.* **2016,** *138*, 4860-4868

III **Kristina Sorochkina**, Vladimir Zhivonitko, Konstantin Chernichenko, Ville-Veikko Telkki, Timo Repo, and Igor Koptyug. Spontaneous N-15 nuclear spin hyperpolarization in metal-free activation of parahydrogen by molecular tweezers, *J. Phys. Chem. Lett.* **2018**, *9*, 903-907

IV **Kristina Sorochkina**, Konstantin Chernichenko, Martin Nieger, Markku Leskelä, and Timo Repo. (Dicyclohexyl(2-(dimesitylboryl)phenyl)phosphine: en route to stable frustrated Lewis pairs-hydrogen adducts in water: *Z. Naturforsch. B* **2017***, 72*, 903-908

V Andrea Hamza,† **Kristina Sorochkina**,† Bianka Kótai, Konstantin Chernichenko, Dénes Berta, Michael Bolte, Martin Nieger, Timo Repo, and Imre Pápai. Origin of stereoselectivity in FLP-catalyzed asymmetric hydrogenation of imines. *ACS Catal.* **2020**, *10*, 14290–14301 († denotes equal contribution)

VI **Kristina Sorochkina**, Konstantin Chernichenko, Vladimir Zhivonitko, Martin Nieger, and Timo Repo. Water reduction and hydrogen addition in aqueous conditions with ansa-phosphinoborane, *under preparation*

The publications are referred to in the text by their roman numerals.

AUTHOR'S CONTRIBUTION

Paper I: The author performed the syntheses, characterizations, and preliminary experiments with dihydrogen under the supervision of Dr. K. Chernichenko and Prof. T. Repo. Dr. B. Kótai, T. Földes and Prof. I. Papai carried out computational work. Assoc. Prof. V. Zhivonitko performed and analysed PHIP experiments with the help of V.-V. Telkki and I. Koptyug, and drafted the manuscript. All authors took part in the manuscript revision.

Paper II: The author performed minor syntheses and analyses. Dr. Chernichenko performed major experimental work with the help of Dr. M. Lindqvist. Dr. M. Nieger performed the X-ray structural analysis. Dr. B. Kótai and Prof. I. Pápai carried out computational work. Prof. T. Repo supervised the study.

Paper III: The author performed synthesis, characterization, and preliminary experiments with dihydrogen under the supervision of Dr. K. Chernichenko and Prof. T. Repo. Assoc. Prof. V. Zhivonitko performed PHIP and thermochemistry experiments and drafted the manuscript. All authors took part in the manuscript revision.

Paper IV: The author performed experimental work and drafted the manuscript under the supervision of Dr. K. Chernichenko and Prof. T. Repo. Dr. M. Nieger performed the X-ray structural analysis. Dr. K. Chernichenko carried out computational work. All authors took part in the manuscript revision.

Paper V: The author performed experimental work under Dr. K. Chernichenko and Prof. T. Repo's supervision and drafted corresponding part of the manuscript. Dr. M. Nieger and Dr. M. Bolte performed the X-ray structural analysis. Dr. A. Hamza carried out computational studies with the help of Dr. B. Kótai and D. Berta. Prof. I.Papai drafted theoretical part of the manuscript. All authors took part in the manuscript revision.

Paper VI: The author performed experimental work under Dr. K. Chernichenko and Prof. T. Repo's supervision and drafted the manuscript. Dr. K. Chernichenko carried out computational studies. Assoc. Prof. V. Zhivonitko performed PHIP experiments. Dr. M. Nieger performed the X-ray structural analysis. All authors took part in the manuscript revision.

ABBREVIATIONS

AAB – *ansa*-aminoboranes
Alk – alkyl
Ar – aryl
Bn – benzyl
bPh – biphenyl
(*t*)Bu – (*tert*-)butyl
CPME – cyclopentyl methyl ether
Cy – cyclohexyl
DABCO – 1,4-diazabicyclo[2.2.2]octane
Dipp – 2,6-diisopropylphenyl
DFT – density functional theory
DQF OPSY – double-quantum filtering only parahydrogen spectroscopy
EC – encounter complex
Et – ethyl
ee – enantiomeric excess
eq. – equivalent
EWG – electron-withdrawing group
ΔG – Gibbs free energy
ΔH – enthalpy change
HIA – hydride ion affinity
HOESY – heteronuclear Overhauser effect spectroscopy
HOMO – highest occupied molecular orbital
*i*Pr – prop-2-yl
Fc – ferrocene
FIA – fluoride ion affinity
FLP – frustrated Lewis pairs
FRP – radical frustrated pairs
GEI – global electrophilicity index
HIA – hydride ion affinity
HSAB – hard and soft acid base theory
I*t*Bu – N,N-di(*tert*-butyl)imidazol-2-ylidene
LA – Lewis acid
LB – Lewis base
LUMO – lowest occupied molecular orbital
MD – molecular dynamics
Me –methyl
Mes – mesityl, 2,4,6-trimethylphenyl
MRI – magnetic resonance imaging
MS – molecular sieves
NMR – nuclear magnetic resonance
Ph – phenyl

PHIP – parahydrogen-induced hyperpolarization
PMP – *para*-methoxyphenyl
ppm – part per million
PTFE – polytetrafluoroethylene
RT – room temperature
(S,S)-diop - 2,3-*O*-isopropylidene-2,3-dihydroxy-1,4-bis(diphenylphosphino) butane
SET – single electron transfer
Ts – tosyl
TBAF – tetra-n-butylammonium fluoride
TMS – trimethylsilyl
TS – transition state
PMP – 4-methoxyphenyl
TMP – 2,2,6,6-tetra-methylpiperidine

1 INTRODUCTION

When combined in the solution, Lewis acid (LA) and Lewis base (LB) usually form Lewis adduct, and, consequently, their reactivity is quenched. However, the formation of Lewis adduct can be precluded by sufficient steric hindrance, preserving acidity of LA and basicity of LB. While this was known since the 1940s,[1] only six decades later, it was discovered that a combination of sterically separated LA and LB can unleash its reactive potential upon heterolytic splitting of σ- and π-bonds (Fig. 1). Such reactivity was translated into a powerful concept known as frustrated Lewis pairs (FLPs).

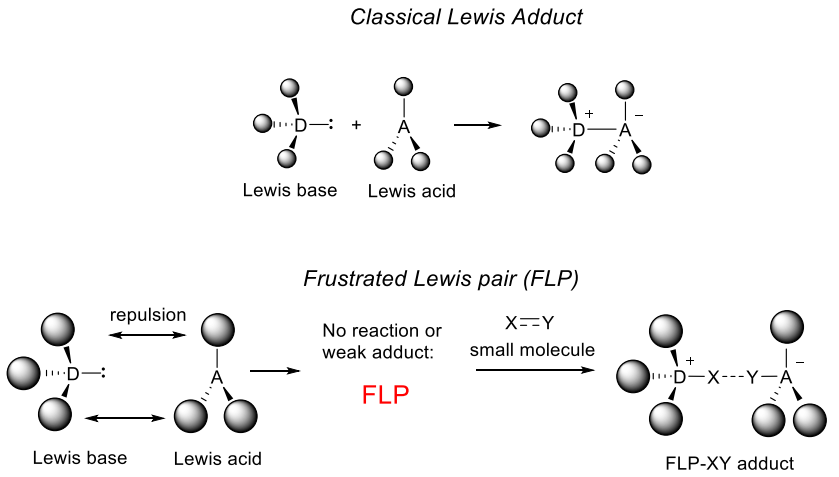

Figure 1 Classical Lewis adduct and frustrated Lewis pair.

The majority of FLPs derive from abundant main group elements and exhibit a spectacular range of reactivities, making them a potential alternative for transition metal catalysis. FLP reaction types can be categorized into 3 classes (Fig. 2):

a) Heterolytic splitting of σ-bonds (Fig. 2, A*).* Such reactivity commonly occurs with sufficiently acidic bonds: H_2, XH (X=halogen, OH, OR), spC-H[2-4] and sp^2C-H-bonds. FLPs also commonly react with hydridic bonds such as B-H bonds of boranes[5, 6] and Si-H bonds of silanes.[7-9] Cleavage of heteroatomic bonds such as C-F,[10, 11] and S-S in disulfides[12] was also reported.

b) Dipolar addition to unsaturated compounds (Fig. 2, B-B'''). 1,2-Addition was reported with alkenes and alkynes, C=O bond containing compounds including CO_2,[13-15] with isothiocyanates,[14] nitroso compounds,[13] and SO_2.[16] 1,3-Addition occurs with N_2O.[17, 18]

c) 1,1-Addition (Fig. 2, C'). Such reactivity was reported with NO,[19] CO,[20] difluorocarbene[21] and azides.[13]

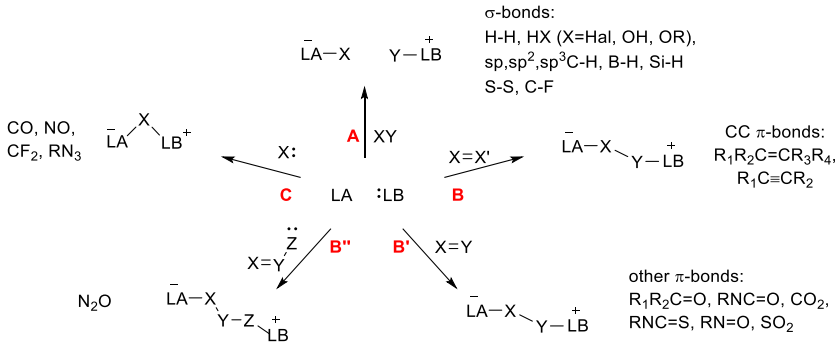

Figure 2 Generalized scheme of FLP reactivities reported to date.

Despite the diverse range of FLP reactivities, only a few were translated into practically important transformations.[22] Among them, hydrogen activation and hydrogenation catalysis[23] are particularly developed.

The landmark discovery reported by Stephan *et al.* in 2006 described the first example of a metal-free system, namely phosphinoborane **1**, which could heterolytically split H_2 in a reversible manner (Fig. 3). Subsequent reports on H_2 splitting by ethylene bridged P/B system **3**[24] and simple combinations of sterically demanding boranes and phosphines[25] or amines [26] demonstrated the generality of the FLP notion. Concurrently, **1** was shown to affect catalytic hydrogenation of bulky imines, aziridines, and protected nitriles[27].

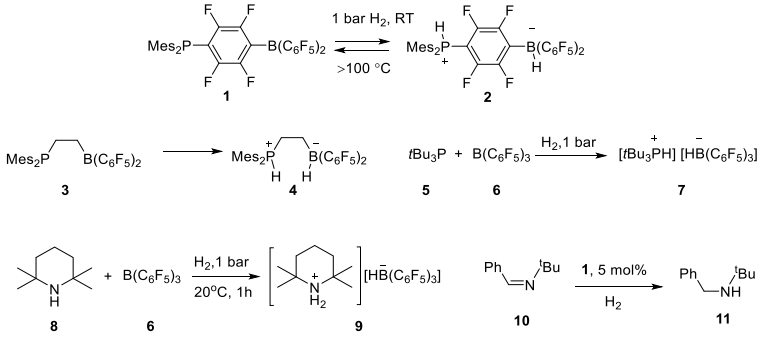

Figure 3 Early examples of FLP reactivity.

Triarylboranes dominate FLP chemistry as Lewis acidic components due to their robustness, hydrolytic stability, and synthetic accessibility. The library of the boranes utilized in FLPs is rapidly expanding,[28] yet, commercial **6** and its derivatives perhaps remain the most common. The range of LAs beyond boranes comprises neutral Al,[29, 30] Ga,[31, 32] In,[31, 32] Sn,[33, 34] cationic borenium,[35]

phosphonium[9], silylium,[36, 37] and methylacridinium[38] species. Lewis bases are typically represented by bulky amines, phosphines and less often by ethereal bases. Examples of more exotic LBs in FLPs include N-heterocyclic carbenes[39, 40] and silylenes.[37, 41] Transition metal-centered LAs and LBs were also actively explored in FLP chemistry.[42, 43]

Besides impressive expansion throughout the periodic table and broadening the scope of transformations enabled by FLPs, the paradigm itself is conceptually evolving. It was realized that sterical "frustration" is not a prerequisite for FLP reactivity. For instance, even robust classical Lewis adducts such as of **6** with Verkade's base $P(MeNCH_2CH_2)_3N$ undergo FLP reactions under ambient conditions.[44] Reactive FLPs can be generated from classical Lewis adducts upon external stimuli such as light or heat, which opens possibility of controlled/switchable reactivity.[45, 46] More recently there has been growing interest in radical frustrated pairs (RFP), a concept that has emerged from the initial observation that single electron transfer (SET) may occur within classical FLP systems.[47] The ability of RFP to operate by a radical mechanism has been already utilized for a few synthetic transformations,[48, 49] and more advances are expected here.[50]

2 SCOPE OF THE THESIS

This work is a continuation of the pioneering research conducted by our group in the field of FLP chemistry. The present thesis focuses on the heterolytic splitting of hydrogen by boron-centred FLPs and its further utilization in 1) NMR signal amplification employing parahydrogen-induced hyperpolarization (PHIP) and 2) asymmetric hydrogenations. Moisture sensitivity of FLPs is one of the major obstacles for their practical implementations, and in particular, for the realization of FLP mediated PHIP in biologically relevant media. Therefore, much work has been directed towards inhibiting interactions of FLPs of our interest with water.

The results and discussion part describes the central findings reported in the attached original publications I-VI. In publications I and II (partly), the family of *ansa*-aminoboranes with altered aromatic substituents at boron site were explored. Publication I discloses a detailed study on their interaction with normal hydrogen and parahydrogen. Here, the common ability of *ansa*-aminoboranes to produce PHIP in a continuous manner is demonstrated, and kinetic and thermodynamic parameters of hydrogen splitting are derived using NMR spectroscopy. In publication II, one of the family members is reported in the context of internal sp^2C-H bond borylation, illustrating the unique ability of such metal-free systems to cleave relatively strong C-H bonds. In publication III, ^{15}N labeled analog *ansa*-aminoboranes were synthesized and subjected to PHIP experiments. Here, substantially higher NMR signal enhancements are achieved due to the replacement of quadrupolar ^{14}N nucleus and spontaneous polarization transfer to ^{15}N nuclei. Publication IV reports *ansa*-phoshinoborane, which does not react with hydrogen or water. Being in sharp contrast with the high moisture sensitivity of N-centred analogs reported in publications I-III, this observation shifted our interest towards P-centred *ansa*-systems. In the publication VI, more Lewis acidic at boron site *ansa*-phosphinoborane is shown to split both hydrogen and water reversibly. It also featured unprecedented stoichiometric reduction of water to molecular hydrogen. The reaction mechanism is investigated by kinetic and computational studies. Finally, in publication V, a highly enantioselective catalyst in the hydrogenation of imines, (+)-camphor-based chiral borane, is reported together with detailed computational studies on the origin of enantioselectivity.

3 LITERATURE REVIEW

3.1 MECHANISTIC BASIS OF H_2 SPLITTING BY FLPS

3.1.1 THERMODYNAMIC CONSIDERATIONS

Due to the simplicity of H_2 splitting by FLPs, its thermodynamic analysis is relatively simple and accurate. Papai *et al.* reported solvent-phase Gibbs free energies (ΔG) of H_2 splitting calculated for a large set of reported inter- and intramolecular FLPs. Calculated ΔG fall in a wide range from +30 to -40 kcal/mol.[51] Computed energies, with few exceptions, are consistent with observed reactivities: negative values were obtained for the reactive systems, and positive (typically above 10 kcal/mol) for unreactive ones, while values for the systems which activate H_2 reversibly lay slightly below zero (-0.1 to -2.5 kcal/mol). The overall process of H_2 addition to non-linked D/A or linked D~A pairs (where D is a donor (LB) and A is an acceptor (LA)) can be split into several chemically meaningful steps. The respective partitioning scheme depicted in Fig. 4 [51-53] includes the following steps: FLP preparation (dative bond breaking), heterolytic H_2 bond cleavage, proton attachment to base, hydride attachment to acid, and stabilizing interactions associated with the formation of ionic pair. Cleavage of H_2 is the most energy consuming step with calculated value of ΔG_{HH} = +128,8 kcal/mol in toluene and is constant for all FLPs. The additional energy ΔG_{prep} is required for dissociation of a weak adduct of LA and LB if such adduct is formed (0-12 kcal/mol for most FLPs).

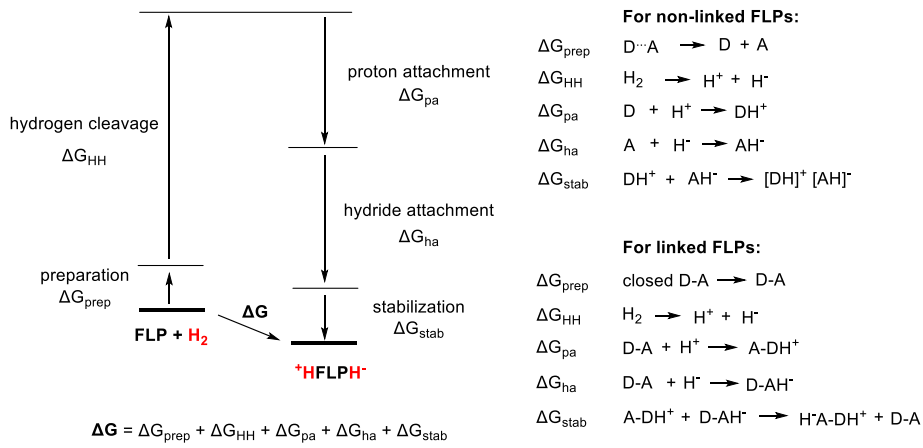

Figure 4 Partitioning of the reaction free energy using Born-Haber cycle formalism. D: donor (Lewis base); A: acceptor (Lewis acid).

These two endergonic steps have to be counterbalanced by the negative energy values of the last three steps to achieve favorable thermodynamics of H_2 cleavage. Protonation of D and hydride attachment to A is the major exergonic steps in the cycle. Corresponding ΔG_{pa} and ΔG_{ha} values are Gibbs free energies of the proton affinity of the donor (PA, basicity) and hydride affinity of the acceptor (HA, hydricity) reflecting on the Lewis donor and acceptor strengths, respectively.

Calculated basicities are plotted on an energy scale in Fig. 5. The values corresponding to conventional amines, phosphines, and their derivatives within linked systems range from -60 to -40 kcal/mol. Carbene I*t*Bu stands out as most basic (ΔG_{pa} = -80 kcal/mol) and least basic $(C_6F_5)_3P$ (ΔG_{pa} = -7 kcal/mol) lies on the opposite edge of the scale.

Reported hydricity values[51, 54] are summarized on an energy scale in Fig. 6. The scale starts from parental $B(C_6F_5)_3$ (ΔG_{pa} = -72.5 kcal/mol), followed by its intramolecular derivatives from the substitution of one p-F with phosphino group. Other intramolecular boranes bearing two C_6F_5 rings lie in a fairly narrow range of ΔG_{pa} = -60 to -55 kcal/mol. In the series of non-linked boranes on the scale, hydricity gradually reduces with decreasing number of halogens in the aromatic rings. In fact, boranes with lower (stronger) calculated hydricity than this of **6** have been reported more recently and discussed in section 3.1.3.

Basicities and hydricities strongly depend on the electron effect of substituents: electron-withdrawing groups increase the strength of LA and decrease the strength of LB; the effect is opposite for electron-donating substituents. In the series, non-linked boranes acidity gradually drops with decreasing number of halogens, but also sterics plays a remarkable role.

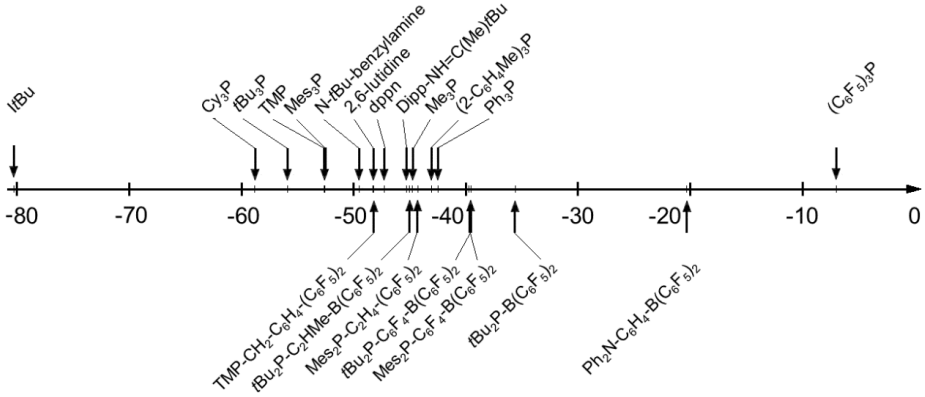

Figure 5 Calculated Gibbs free energies of proton attachment to the Lewis donor. [51]

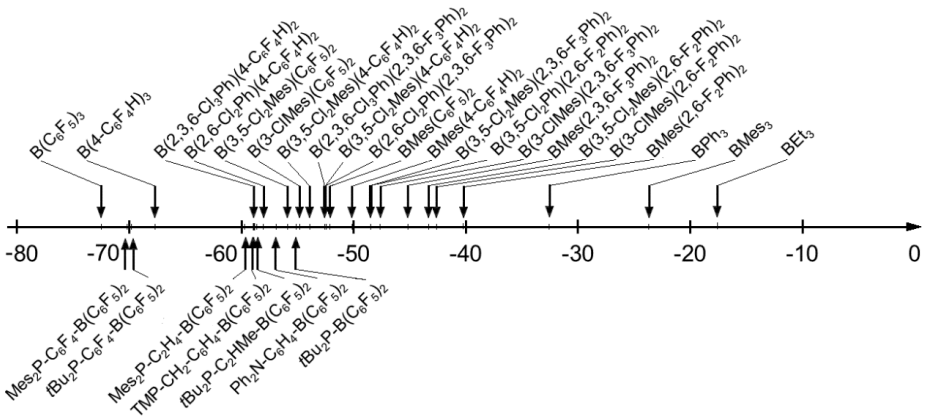

Figure 6 Calculated Gibbs free energies of hydride attachment to the Lewis acceptor. [51, 54]

The final term ΔG_{stab} represents Gibbs free energy of the formation of ion pair from separated ions DH^+/AH^- or $A{\sim}DH^+/D{\sim}AH^-$. For intermolecular systems it is binding free energy, including a positive entropic term as two ions associate into one ionic complex. Quantitative analysis ΔG_{stab} values account for a narrow range of -14 to -24 kcal/mol presumably due to the structural similarity of the considered pairs (neutral charge, shielding bulky substituents, narrow distribution of distances d_{DA}). For intermolecular systems stabilization effect ΔG_{stab} is thought to be an interplay of multiple weak interactions, such as electrostatics, dispersion, repulsion, solvation effects, etc. For instance, weak correlation between ΔG_{stab} and reciprocal distances $1/d_{DA}$, observed in the gas phase, becomes undetectable in the solvent phase. For intramolecular systems ΔG_{stab} is reasoned differently; namely, it measures how much hydride attachment enhances basicity (D~A vs. D~AH-), and proton attachment enhances acidity (D~A vs. A~DH+), reflecting acid-base cooperative effect. Stabilization interaction ΔG_{stab} of the linked systems falls in a broader range (-21 to -65 kcal/mol) and is substantially stronger. Such difference is presumably attributed to the aforementioned cooperative effect and smaller entropic loss: in the last step number of species does not change, unlike for intermolecular systems. Additionally, ΔG_{stab} showed a linear correlation with $1/d_{DA}$, pointing that the acid/base cooperation is distance-dependent.

This analysis revealed the fundamental difference between inter- and intramolecular systems: for the former (unless they form a dative complex and somewhat resembles intramolecular case), thermodynamics is determined by cumulative acid-base strength, while for later, ΔG_{stab} makes a significant contribution and can even become a decisive factor for overall thermodynamics. This peculiarity was utilized in the design of intramolecular FLPs with substantially less acidic boryl sites.[55]

3.1.2 KINETIC CONSIDERATIONS

Direct kinetic exploration of FLP reactions with H_2 due to experimental constraints related to adding gaseous and poorly soluble H_2 to the reaction mixture and controlling its concentration; eventually, the reaction rate can become diffusion controlled. For this reason, mechanistic views on hydrogen splitting and hydrogenation pathways primarily rely on computational studies.

Splitting H_2 by non-linked FLPs involves three molecules and is typically rapid under mild conditions. Due to the low probability of termolecular collision scenario, the process was postulated to be stepwise, comprising the association of two reactants before the reaction with the third. The possibility of binary interaction binding of H_2 to borane or a base (phosphine) has experimental grounds. Adducts $H_2 \cdots BH_3$[56] and $R_3P \cdots H_2$[57] were detected in an argon matrix. Activation of H_2 in some cases occurs in the absence of base: as with antiaromatic boroles,[58, 59] or with boranes $(MesF)_2BD$,[60] $DB(C_6F_5)_2$ and BD_3-THF[61], which undergo D/H exchange under H_2 pressure to form analog hydroboranes. However, mechanistic investigations accompanying these examples suggest that observed reactivities arise from specific structural features and can not be generalized for all FLPs.

Computational studies of prototypical reaction **5**/**6**+H_2 in the gas phase revealed that H_2 interactions with either borane or phosphine are repulsive. Rather loosely bound complex **5**···**6** (Fig. 7), known as encounter complex (EC), was located at the minima of the potential energy surface.[62] The EC is characterized by P-B distance 4 Å and weak overlap of P/B frontier orbitals. The association energy was found to be 11-15 kcal/mol, depending on the level of calculations,[62-65] and arises from multiple weak C-H···F interactions and dispersion forces (presumably lp-π interaction between phosphorus lone pair and C_6F_5 ring)[63]. Varying P-B distance within the range of 3.7 -4.7 Å corresponds to only 2 kcal/mol interval on the energy scale, reflecting the high structural flexibility of the EC.

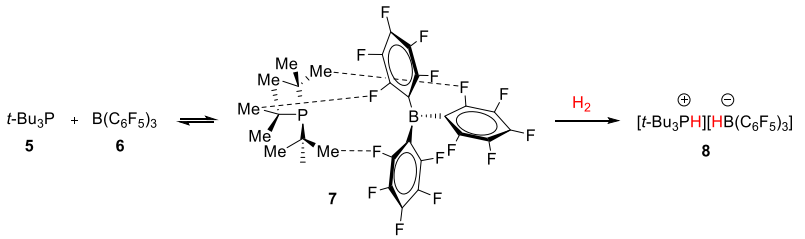

Figure 7 Preassociation of FLP components into EC is proposed to rationalize high reactivity towards H_2.

The second step of the process is hydrogen splitting. For the **5**/**6** +H_2 system, a single early transition state TS1 (TS) was located 10.4 kcal/mol above reactants EC+H_2.[62] It featured nearly linear PHHB unit and maintained CH···F

and van der Waals contacts between the phosphine and borane molecules as in EC. A later study on **5**/**6** and other FLPs conducted at higher level of theory provided more accurate structural parameters for corresponding TSs; in particular, the PHHB unit appeared to be L-shaped (Fig. 8).[66] All computed TSs [52, 62, 64, 66] feature the following geometry: 1) H_2 molecule is slightly stretched, suggesting an early TS (0.77-0.99 Å) 2)D···H (where D is P- or N-centered donor) and H···B distances shorter than the sum of van der Waals radii, meaning that H_2 interacts simultaneously with donor and acceptor centers 3) DHH unit is nearly linear and HHB unit notably bent 4) borane unit is pyramidalized. Analysis of the TS electronic structure revealed notable HH bond polarization featuring bond orders 0.7-0.8. From a molecular orbital point of view synergetic electron transfer from lone pair orbital of the Lewis base to $\sigma^*(H_2)$ and from $\sigma(H_2)$ to the empty orbital of the Lewis acid, leading to polarization, weakening and ultimate heterolytic HH bond cleavage. Thus, H_2 molecule acts as a bridge between the phosphine and borane fragments, enabling an electron transfer that was prevented in the frustrated complex.
Presumably, the preorganization of active sites and flexibility of the EC ensures its rapid interaction with upcoming H2. Calculated activation barriers are quite low: 0-8 kcal above EC+H_2 for most of the calculated TSs. The distortion of EC accounts for only a minor contribution to activation energy (2.4 kcal out of the total activation energy of 7.4 kcal), and the rest arises from the work required for hydrogen diffusion in the EC cavity (distort the three fragments and to create the orbital overlaps) and therefore is entropy controlled.

Whether or not EC represents an actual reactive species is still debatable. Classical MD simulations pointed that EC in toluene is unfavorable, yet, it is presented at 0.5% concentration.[67] In the solution, the stabilizing interactions within EC are significantly weaker, and it does not exhibit preferential orientation.[68] Based on MD simulations, the pair 2,6-lutidine/**6** exist in

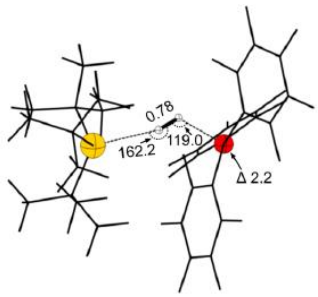

Figure 8 Transition state for the system tBu$_3$P + B(C$_6$F$_5$)$_3$ + H_2

separated solvent cages rather than in the associated form.[69] Nevertheless, experimental evidence of EC formation was offered by neutron scattering and NMR studies in ionic liquids.[70] Combined ^{19}F, ^{1}H HOESY NMR studies provided further evidence of association of Mes_3P/**6** or tBu_3P/**6** in the solution based on observation of C-H···F interactions.[71] These associates, however, did not feature preferential orientation.

Recently direct kinetic study of H_2 activation with Mes_3P/**6** by isothermal calorimetry has been reported.[72] Obtained experimental data could be well modeled as a single termolecular reaction with the rate constant 0.61 M^{-2} s^{-1} at 303 K. However, the identical rate law would apply for the pathway involving an EC, assuming that the encounter complex formation is a rapid equilibrium prior to the rate-determining H_2 activation step:

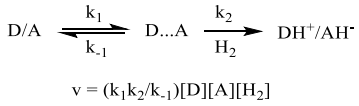

Figure 9 Two-step activation of H_2 by FLP and the associated rate law.

Determination of activation parameters revealed that the reaction is entropy controlled. At the same time, virtually no kinetic isotope effect was observed in the experiments with D_2. Together, these observations suggest that the diffusion of H_2 into the "encounter complex pocket" is an actual rate-limiting step, that is followed by hydrogen cleavage. Enthalpic barrier was found as small as $\Delta H^{\ddagger}$ = 3.3 kcal mol^{-1} * $\Delta G^{\ddagger}$= 17.7), yet its non-zero value indicates that the reaction proceeds via the transition state.

In the view of EC concept, intramolecular FLP with spatially close active centres represents a particular case of such, which brings kinetic advantage in the reaction with H_2.

3.1.3 ALTERING LEWIS ACIDITY

Energy partitioning analysis illustrated the importance of quantification of LA and LB strengths for rational FLP design. In a big portion of FLP reactions, including hydrogen splitting, LB accepts a proton, and its strength can be well correlated with proton affinity (PA) or Brønsted basicity in the solution, of which tabular values are widely available. In contrast, there is no universal choice of Lewis acidity scale. Commonly employed metrics are defined with respect to complementary bases, that vary significantly in their nature. Therefore, it is essential to compare these metrics and understand their limitations.

Assessment of Lewis acidity by spectroscopic methods (Fig. 10) is widespread. Gutmann-Becket method measures Lewis acidity (Gutmann number NA) based on the change in ^{31}P NMR chemical shift of Et_3PO upon

coordination with LA[73, 74] (Fig. 10) Childs method utilizes crotonaldehydes as the complementary base and assesses ^{1}H NMR chemical shift of H^{3} proton upon complexation with LA[75]. Computational measures of Lewis acidity (Fig. 10) derive thermodynamic parameters of adduct formation between LB and LA in question. For instance, hydride affinity (HA) and fluoride ion affinity (FIA) calculate the enthalpy change upon binding of H^- or F^- correspondingly to LA in question in a gas phase via isodesmic reactions.[76, 77] Naturally, these methods can be used in a predictive manner.

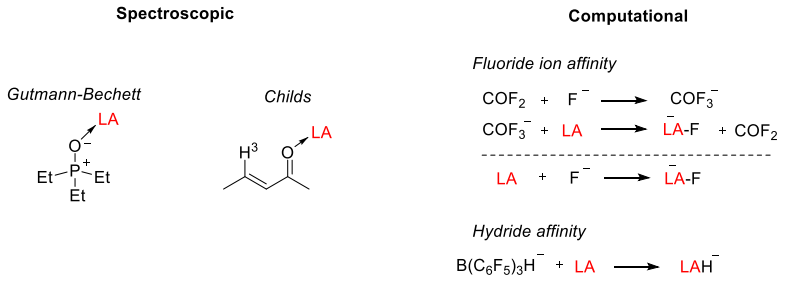

Figure 10 Methods for determination of the Lewis acidity.

The ability of LA to accept electron density without regard to a particular base can be evaluated based on electrochemically measured reduction potential.[78, 79] Global Electrophilicity Index (GEI, ω) is another intrinsic Lewis acidity metric,[80, 81] which is defined as $\omega = \chi^2/2\eta$, where χ electronegativity, and η is hardness. Both χ and η values can be derived from computed one-electron energies of the frontier molecular orbital E_{HOMO} and E_{LUMO} of the optimized LA structure. Hence, GEI represents a "cheaper" computational method than FIA and HIA, where structural optimizations of several species are needed.

Attenuation of Lewis acidity is a common strategy to achieve compatibility of FLP systems towards polar functional groups; besides, upon H_2 activation less acidic boranes give intermediates, that are stronger hydride donors. This facilitates the subsequent hydride transfer step. In this context number of tempered boranes achieved by simply F/H replacements in parental **6** were explored in the past years. [82-88] Recently, Stephan *et al.* systematically assessed Lewis acidities within the library of 20 partially fluorinated analogs of **6** by GEI (Fig.11, compounds **9**). The latter nearly linearly correlated with an absolute number of fluorines in the structure; however, slight deviations were observed depending on the position of F atoms: those in *meta* position have slightly stronger electron withdrawal effect than in *para* positions. Importantly, boranes with the same number of *ortho, meta,* and *para* F have the same GEI regardless of their distribution among the rings, which is valuable insight from a synthetic point of view. This study also revealed that, given that steric congestion around boron is the same, GEI is in good

agreement with Childs scale, while FIA scale - with Gutmann-Becket scale, which was rationalized by HSAB theory.

Generation of stronger Lewis acidic boranes than **6** appeared to be a challenging task. Fluorine has the strongest positive inductive effect among halogens, however, its back-donation of lone electron pair to the aromatic system is also prominent. Hammett parameter, which reflects combined mesomeric and inductive effect of the substituent, is substantially greater for Cl (σ_{para}=0.23) than F (σ_{para}=0.06)(more positive value denotes greater electron withdrawing group). Investigation on the electronic structure of the series $B(C_6F_5)_{3-n}(C_6Cl_5)_n$, n = 0-3 (**6**, **10a-c**, Fig.11) confirmed that boron atom becomes more electron deficient concurrently with the replacement of each C_6F_5 with C_6Cl_5 according to ^{11}B NMR chemical shifts, computed electron charges on B atom, and reduction potentials measured by cyclic voltammetry.[79] In the later work, calculated HIAs energies for **10b** and **10c** were found to be 0.4 and 1.1 kcal lower relative to **6** (stronger affinities).[89] In contrast, Lewis acidity estimated by Guttmann-Beckett and Childs methods within the series **10a-c** followed the opposite trend due to the increasing steric hindrance.[79] Repulsion with bulkier Cl around boron center upon interaction with bigger donors (front strain) and higher energetic costs for pyramidization of B center caused by repulsion of sterically bulky C_6Cl_5 fragments at the back (back strain) disfavor B-O bond formation.

Even for a smaller donor like H_2O, contribution of sterics to Lewis acidity overrides electronics: unlike **6**-H_2O, its bulkier homolog **10a** releases water under vacuum or in the solution upon addition of molecular sieves and pristine **10c** could be recovered after refluxing in a toluene/H2O mixture for several days. These observations illustrate the basis for the size-exclusion principle in FLP design: steric modulation around boron to discriminate donors by size. Since H_2 is the smallest possible molecule, such an approach can inhibit interaction of borane with other donors without compromising on reactivity towards H_2.

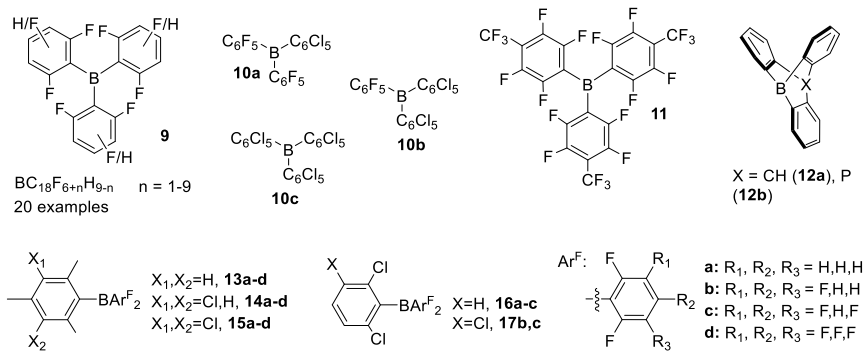

Figure 11 Highly Lewis acidic boranes.

Recently Mitzel *et al.* reported a super Lewis acid, the tris-(perfluorotolyl) borane **11** (Fig.11).[90] Replacement of F with stronger electron acceptor CF_3 (σ_{para}=0.54) in the *para*-positions of **6** does not impose energetic penalties associated with the front and back strains compared to **6**. Guttmann-Beckett and FIA values of **11** were found to be about 10% higher than those of **6,** and HIA was found 12.6 kcal stronger. Substantial enhancement of Lewis acidity can be achieved by rendering pyramidalization of planar trivalent B centre. Thus, Lewis acidities of non-halogenated boranes **12a** and **12b** evaluated by the HIA scale are comparable to those of **6**, and are slightly stronger according to the FIA scale. [91]

Size-exclusion design was successfully applied in the development of functional groups and moisture tolerant boranes. In the related work, [54] Soós and Pápai systematically investigated the broad series of halogenated triarylboranes BYX_2 (**13-17**, Fig.11) with default steric congestion around boron: Y ring bears at least two Cl or two Me (those two substituents are isosteric) in ortho-position, and each X ring bears at least two ortho F substituents. Calculated gas-phase HIAs plotted against the number of F in the X ring for each small series (**13 a-d, 14 a-d, 15 a-d, 16 a-c, 17b,c**) gave nearly linear trends with about 5kcal step for each additional F on X ring with more prominent effect at *meta*-positions. Interestingly, that H/Cl replacement in the Y ring affected HA to less extend, presumably because of the lower level of the conjunction of B center with bulkier aromatic ring, which is forced perpendicular to *ipso*-C atoms.

3.2 FLP CATALYSED HYDROGENATIONS

3.2.1 HYDROGENATION OF DOUBLE BONDS

Since the products of H_2 splitting by FLPs possess ionic character, FLPs were explored as catalysts in hydrogenation of polar substrates at first, including imines, N-heterocycles, enamines, silyl ethers, enones, and ynones. The FLP hydrogenation catalyst may comprise both LA and LB components, separated or linked, or a single LA. Shortly after the first report on FLP-catalysed hydrogenation by **1**, it was discovered that **6** alone could catalyse the reduction of sterically hindered imines and N-heterocycles [92-95]. These early reports postulated the mechanism where the substrate functions as a basic component giving iminium hydroborate pair upon H_2 splitting with borane (Fig. 12, Cycle A). Subsequent hydride transfer from boron to iminium carbon yields amine-borane adduct, dissociating to release free borane and the product. Since the latter is also a viable base for hydrogen activation, the process might occur through the autoinduced catalytic cycle (Fig. 12, Cycle B, where the base is the produced amine). Paradies *et al.* showed that whether hydrogenation proceeds via catalytic cycle A or B is determined by Lewis acidity of borane.[96, 97] While **6** is unselective with regard to Lewis base (imine or amine), catalysis with less

acidic boranes **9a** $B(2,6\text{-}F_2Ph)_3$ and **9b** $B(2,4,6\text{-}F_3Ph)_3$ proceeds via autoinduced cycle B due to higher activation energies (2 kcal mol^{-1}) for H_2 splitting by the imine *versus* amine.

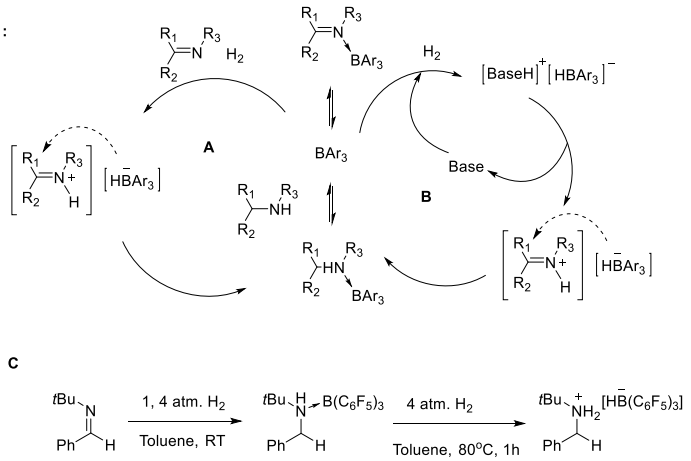

Figure 12 (A) Catalytic cycle induced by imine and (B) Catalytic cycle induced by external base or produced amine (autoinduced process). (C) Hydrogenation of bulky imines

Stoichiometric reaction between imine-borane pair and H_2 occurs at room temperature, but further activation of H_2 by formed amine-borane adduct requires heating due to high dissociation energy. Thus, hydrogenation of imines,[92, 93] or N-heterocycles such as substituted quinolines, phenanthroline, acridines[94], indoles[93, 95] catalysed by **6** proceeds with sufficiently hindered substrates at elevated temperatures (Fig. 13a,b). Naturally, strong binding with amine and other functional groups present in the system can hamper or completely quench catalyst activity. To overcome this limitation, Soós *et al.*[98, 99] exploited the size-exclusion principle in the design of hydrogenation catalyst comprising sterically shielded $MesB(C_6F_5)_3$ (**13d**) and DABCO (**20**) or quinuclidine (**21**), compact bases that could ensure H_2 activation regardless the substrate nature. These catalytic systems enabled hydrogenations of double bonds of sterically accessible imines, enamines and enones at room temperatures and featured high functional group tolerance and chemoselectivity. (Fig. 13, c). More chemically robust borane modification **13c** broadened substrate scope to sterically accessible quinolines and, notably, retained activity after exposure to air. The reduction could be accomplished without an external base at elevated temperature (Fig. 13, d).

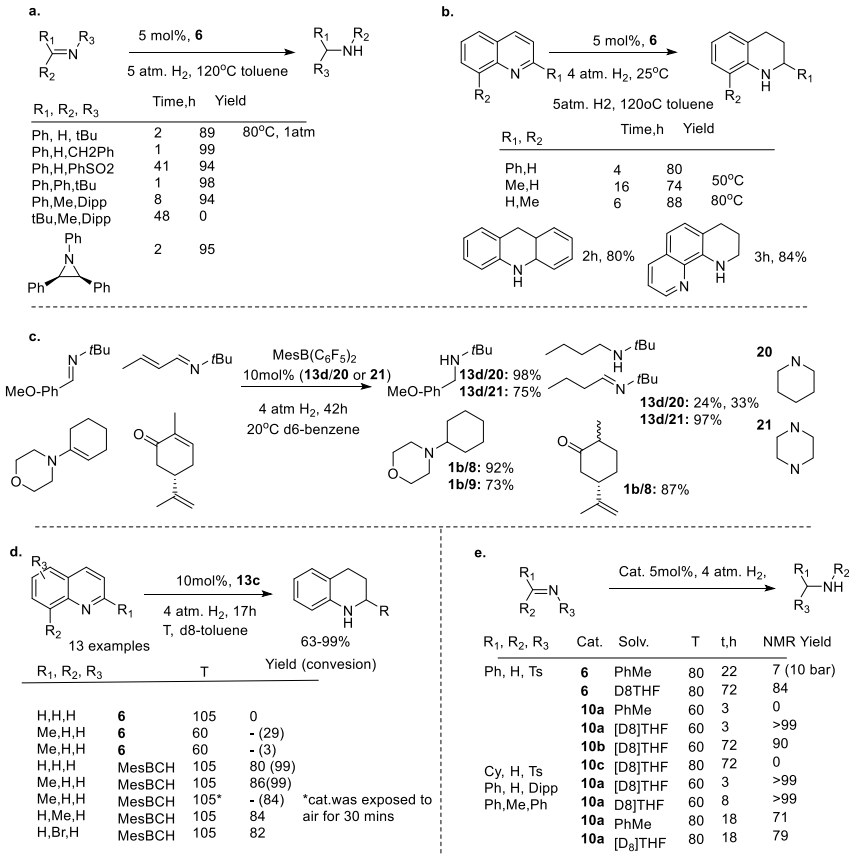

Figure 13 Hydrogenation of polar substrates catalysed by FLPs.

The use of single component borane **6** as a catalyst is appealing but limited by the basicity of substrates/product: hydrogenation of substrates with diminished basicity requires forcing conditions or auxiliary base. Anticipating that the strong-donor solvent can operate as a base, Ashley *et al.* probed sterically shielded boranes $B(C_6F_5)_{3-n}(C_6Cl_5)_n$, n = 1-3 (**10a-c**,) in the hydrogenation of imines in THF (Fig. 13, e). [79] Among the series, **10a** was found to be particularly effective, while **10c** did not show any reactivity, presumably due to excessive steric bulk. As was discussed previously, **10a** is more Lewis acidic with respect to hydride and at the same time less acidic with respect to O-donors compared to **6.** Hence, weakly bound pair **10a**/THF is capable of hydrogen activation under mild conditions, upon which highly Brønsted acidic protonated THF is formed. This allowed hydrogenation of the weakly basic imines, furans, pyrroles. Air stability of **10a** and utilization of "greener" polar solvent which enables solubilising of a broader range of potential substrates, make the protocol especially handy.

FLPs with properly prearranged LA-LB centres can be considered as 100% EC. As this kinetic advantage results in facile hydrogen splitting, they were expected to be superior catalysts over intermolecular counterparts. Indeed, one of the first intramolecular systems reported by Erker *et al.,* ethylene-bridged **4** (Fig. 14), appeared to be far more active in the hydrogenation of imines and enamines than the previously reported FLP catalysts.[100] For instance, hydrogenation of imine **7** occurred at room temperatures under 2.5 atm H_2 in 3 hours. On the other hand, **22** reacts with H_2 instantly to form an adduct **22-H₂**, but the latter poorly performed as a catalyst in the hydrogenation of imines.[101] Later, various intramolecular systems (**23-28**) were reported to effect hydrogenations of imines and enamines,[102-106] yet again not overperforming activity of non-linked systems. Presumably, the energetic disadvantages of hydrogen transfer from the intramolecular hydrogen adducts hamper catalyst activity despite facile H_2 splitting.

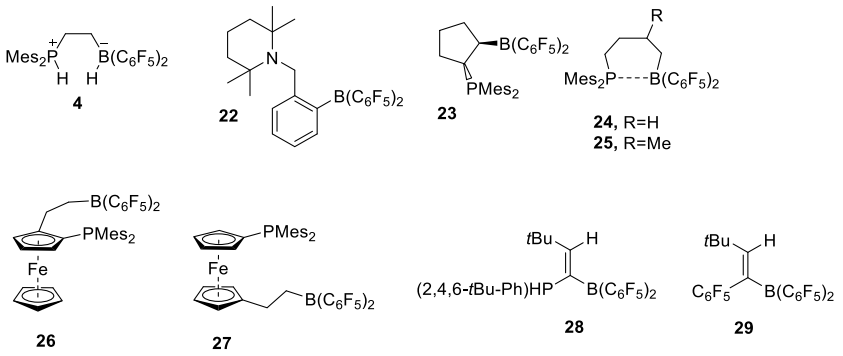

Figure 14 Intramolecular FLP hydrogenation catalysts.

Like for imines, hydrogenation of enamines and silyl enol ethers occurs via activation of carbonyl group by protonation, followed by hydride attack on activated carbon. Reduction of enamines was effected by catalysts **4**, [100] $MesB(C_6F_5)_3$ (**13d**) /DABCO, [98] **22-28**.[101-106] Hydrogenations of poorly basic silyl enol ethers typically requires FLP catalysts comprising an auxiliary base, such as commercially available phosphines in combinations with **6**.[106-108] FLP-promoted reduction of enones and ynones occurs in the reverse order than that for imines: hydride transfer to Michael position is followed by protonation. Hence, generation of more nucleophilic hydroborate species derived from less Lewis acidic boranes facilitates the reaction. Borane **13d** effected hydrogenation of activated double bond of carvone to dihydrocarvone,[98] and borane **10a** hydrogenated CH2=CHC(O)O*n*-Bu in THF.[109] Erker *et al.* reported **29** in combination with DABCO as effective catalyst for the reduction of ynone and a small series of enones.

3.2.2 ASYMMETRIC HYDROGENATION

Remarkable efforts were dedicated to the development of an asymmetric version of hydrogenation catalysis with FLPs (Fig. 15, 16). From a practical point of view, steric induction by LB is an attractive approach as plenty of bench stable chiral amines and phosphines are readily available. However, hydrogenation of PhCMe=NPh employing commercial chiral phosphines in combination with $B(C_6F_5)_3$ resulted in only 25% ee when (S,S)-diop **30** was used.[95] Reaction required prolonged heating at 100°C, which likely diminished the enantioselectivity. Unproductive attempts to employ chiral bases in FLP hydrogenations can be rationalized from mechanistic point of view. In the corresponding catalytic cycle (Fig. 12) hydride transfer to prochiral imine is an enantioselectivity determining step, and it does not involve base directly. Additionally, imine or amine can be involved in the competing autoinduced process, decreasing enantioselectivity.

Generation of chiral (at boron) intermediate borohydrides then should be a more efficient strategy, but due to the trigonal geometry of boranes and limited choice of substituents dictated by the Lewis acidity requirements, it is practically hard to implement.[110, 111] Instead, Lewis acidic boron center is typically installed on the chiral backbone. The first FLP-type asymmetric hydrogenation was reported by Klankermayer *et al.,* employing (+)-α-pinene derived borane **31** as a sole catalyst.[93] Imine PhCMe=NPh **32a** was reduced with full conversion under relatively mild conditions, albeit with only 13% ee. Subsequently, enantioselectivity was substantially improved by employing **35a** derived from (1R)-(+)-camphor scaffold. Hydroboration of alkene **33** with Piers' borane **34** gave a diastereomeric mixture of boranes in the ratio 1÷4. They could be separated upon hydrogen activation in the presence of tBu$_3$P via kinetically controlled crystallization, as adduct **35b** forms faster than **35a**. In hydrogenations of imines **35a** showed poor ee while **35b** provided products with up to 99% yields and up to 83% ee. Its intramolecular analog **36**[112] was obtained as exclusive stereoisomer after the hydroboration step. Catalyst **36** gave lower enantioselectivities than **35b**, but, interestingly, its zwitterionic hydrogen adduct featured high stability and could be recycled 5 times without loss of enantioselectivity.

Intramolecular *ansa*-aminoboranes were found to be active hydrogenation catalysts under mild conditions (room temperature), which is essential for achieving high ees. Therefore, their analogs bearing chiral amine moieties were probed in the hydrogenation of imines.[113] Rigid and bulky chiral amine moiety in the structure of ansa-ammonium borane **37** was expected to ensure generation of chiral at nitrogen ammonium center with high enantioselectivity. Nevertheless, **37** obtained upon the reaction of corresponding *ansa*-aminoborane with H_2 was isolated as a mixture of two diastereomeric hydrogen adducts, indicating low asymmetric induction already at the hydrogen activation step. In hydrogenation experiments, **37** reached 35% ee for imines and 37% ee for quinolines at most. In contrast, chiral intramolecular *ansa*-ammonium borate **38** based on a binaphthyl

scaffold was proved to be highly selective in the hydrogenation of a wide range of structurally different substrates at mild conditions.[114] The catalyst was particularly effective in the hydrogenation of acetophenone, N-alkyl and -benzyl imines (76-83% ee) and enamines (47-99% ee), giving excellent conversions.

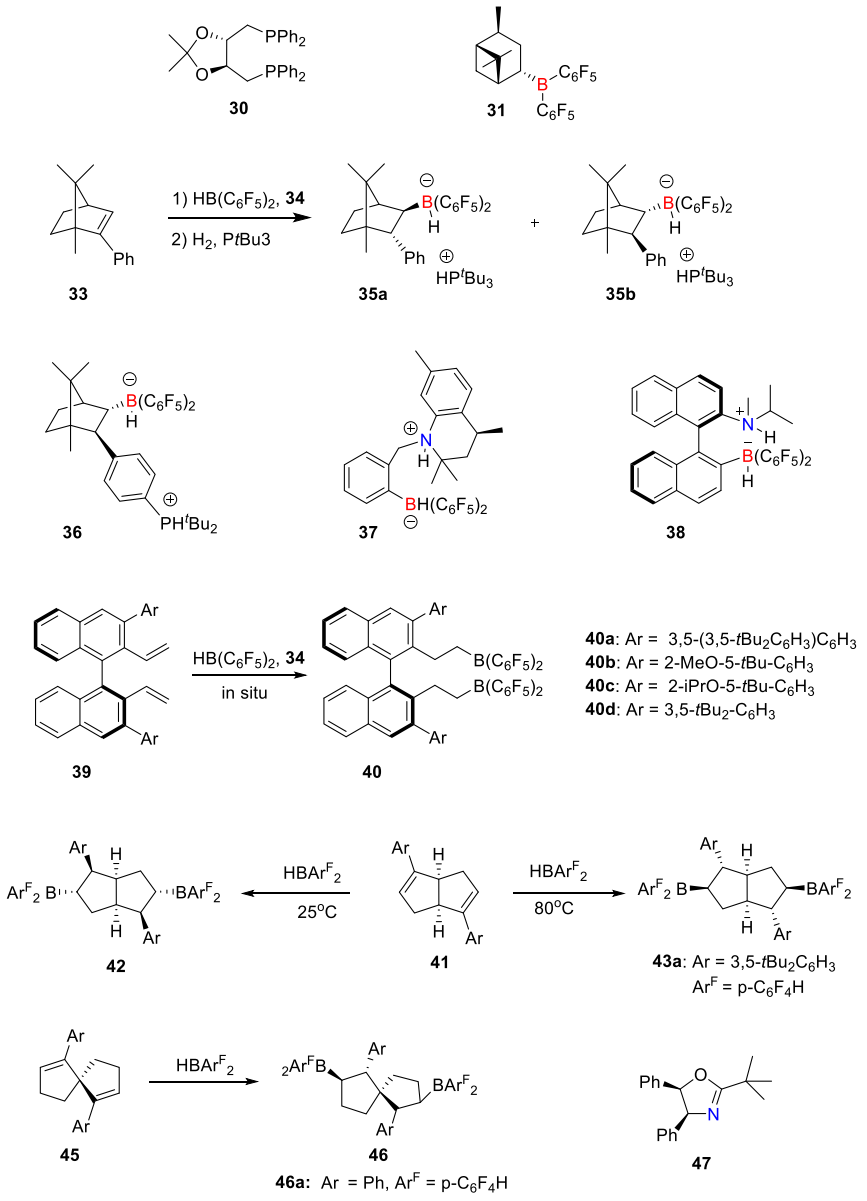

Figure 15 FLP catalysts for chiral hydrogenation.

Du et al. developed a family of efficient FLP catalysts bisboranes **40** derived from the axially chiral 1,1´-binaphthyl scaffold. [115] Bisboranes **40** can be cleanly generated by hydroboration of corresponding terminal bis-alkenes **39** with **34a**. The catalyst can be assembled *in situ*, which eliminates the necessity for tedious isolation (separation of diastereomers), storage, and handling of the moisture sensitive organoboranes. Screening of the wide palette of 3,3′-diaryl substituted bisboranes in the hydrogenation of model imine **32a** revealed that enantioselectivity is sensitive to the bulkiness of the Ar substituent.[116] The most sterically hindered bisborane **40a** gave the highest ees, and further screening with various imines at mild conditions (20 bar, room temperature) gave ees in the range of 74-89% and high conversions (63-99%). The results are similar to those obtained for **35a**, albeit broader substrate scope was explored bearing halides and ethers. Bisboranes **40** were successfully applied in stereoselective hydrogenations of polysubstituted N-heterocycles such as 2,3-disubstituted quinoxalines using **40b**,[117] 2,3,4-trisubstituted quinolines using **40c**,[118] 2,3 - and 2,4-disubstituted quinolines using **40b**,[119] and others.[120] Highly enantioselective hydrogenations of silyl enol ethers were achieved with **40b** in combination with external base tBu$_3$P (**5**).[121] Corresponding secondary alcohols were obtained after deprotection by TBAF in excellent yields (93-99%) and enantiopure almost in all cases.

Wang *et al.* introduced a family of C_2-symmetric bicyclic bisboranes prepared by hydroboration of internal diene **41** with **34a** or its analog HB(p-$C_6F_4H)_2$ **34b**.[122] Diastereomers **42** and **43** could be selectively prepared from **41** depending on the temperature. Generated *in situ* at 80°C **43a** afforded hydrogenations of imines with excellent activity (turnover number is up to 200) and enantioselectivity (up to 95% ee) at -40°C and thus outperformed catalysts **35a** and **40a**. Subsequently, the same group reported a series of spiral-bicyclic bisboranes **46**. *In situ* generated **46a** was particularly selective in the hydrogenation of 2-alkyl, -vinyl, and -allyl substituted quinolines. Enantioselective reduction 2-aryl and 2-hetaryl substituted quinolines was achieved with the combination of **46a** / P(3,5-$(CF_3)_2$Ph)$_3$.

The long-standing problem of asymmetric hydrogenation of carbonyl compounds has been resolved recently by using achiral boranes in combination with chiral oxazoline **47**, thus, representing a rare example of successful utilization of chiral base to induce chirality in FLP catalysed reductions.[123] Ketones were reduced to corresponding alcohols using B(p-$C_6F_4H)_3$(**9c**)/**47** in 43–97% yields with 50–87% ee. Hydrogenation of enones and chromones to ketones was achieved in high yields and up to 95% ee.

In addition to direct hydrogenation, other types of FLP-catalysed asymmetric reductions such as hydrosilylation and transfer hydrogenation were successfully explored.[120]

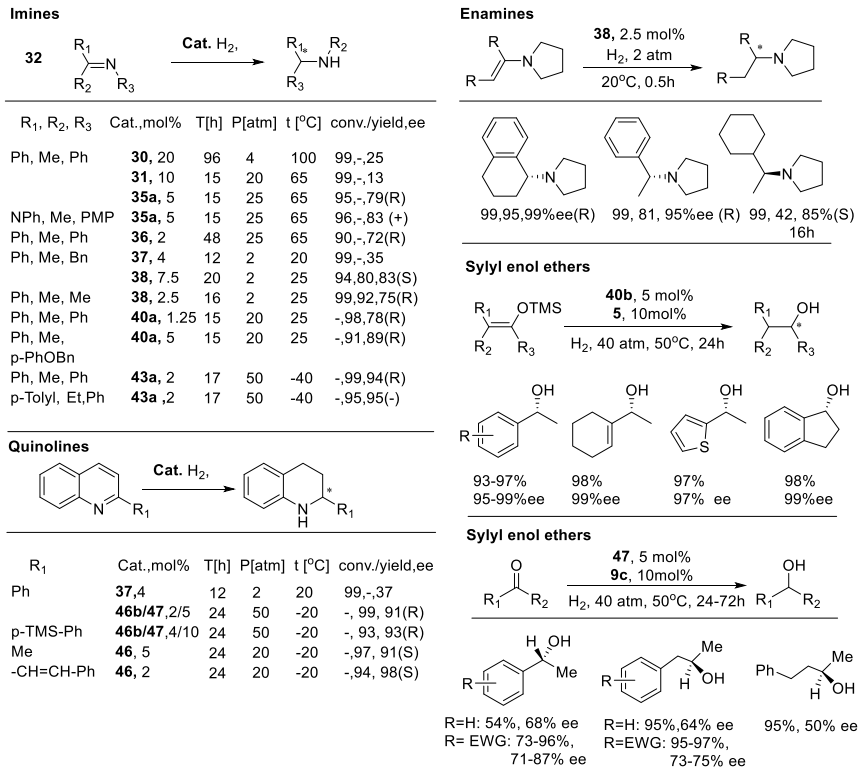

Figure 16 Asymmetric FLP catalysed hydrogenations of polar double bonds.

3.3 HYDROGENATION OF C=O BONDS AND WATER TOLERANCE

Commercially available $B(C_6F_5)_3$ (**6**),[124, 125] is a strong Lewis acid, somewhat between BCl_3 and BF_3,[126] but possesses the substantial steric bulk, is thermally robust, and moisture stable compared to boron halides. In fact, some reactions catalysed by **6** can be carried out in aqueous solutions. [124, 125, 127] In FLP-type reactions when combined with strong bases such as phosphine or amine, **6** exhibits high functional group sensitivity, especially towards O-H bonds. Marked inhibition occurs through H_2O coordination to form complex **6**-H2O, which, being a very strong Brønsted acid, [126] in the presence of strong LB, is further deprotonated to an ion pair [**6**-OH]-[LBH]+ (Fig. 17, a). While the formation of **6**-H2O is reversible, its deprotonation is typically not. Even without base upon heating complex **6**-H_2O undergoes protodeboronation to form **48** induced by proton transfer from the coordinated water to C_6F_5 substituent.

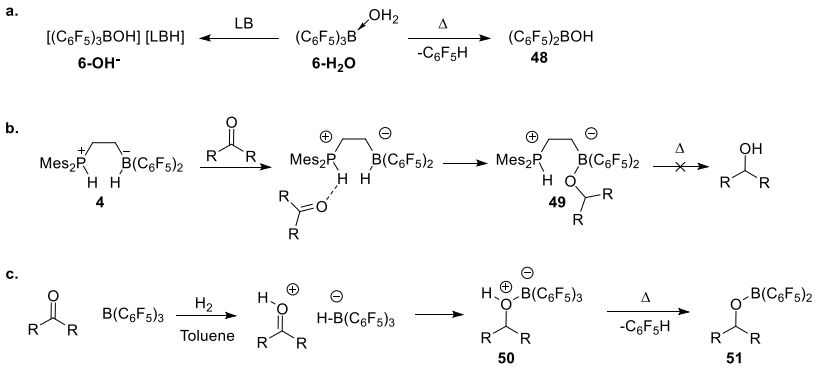

Figure 17 Deactivation of FLPs by (a) water or (b,c) ROH.

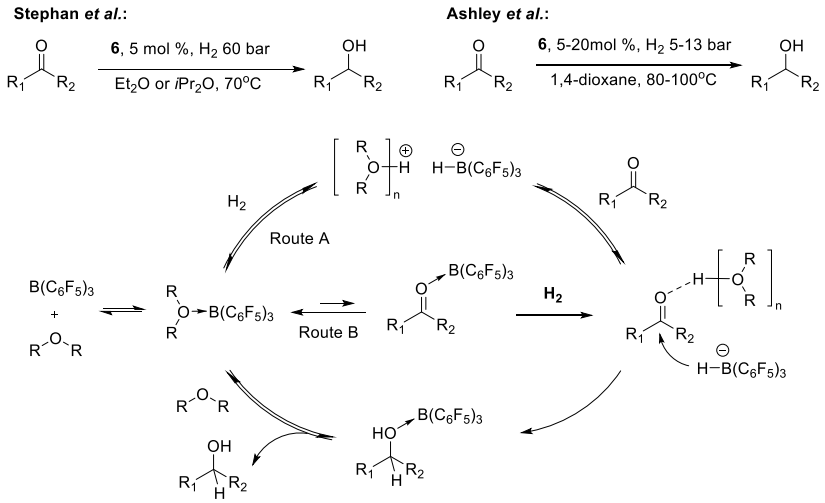

Figure 18 FLP-mediated hydrogenation of carbonyl compounds and proposed mechanism. R_1 -aryl, alkyl, R_2 – alkyl, H.

FLP's deactivation appeared to be an obstacle in the hydrogenation of carbonyl compounds. The reaction of phosphonium borohydride **4** with the ketone led to its reduction and concurrent irreversible formation of FLP adduct with the produced alcohol (Fig. 17, b). Theoretical studies suggested feasibility of the direct H_2 activation by ketone or aldehyde/**6** pairs.[128, 129] Indeed, experimental attempts to hydrogenate carbonyl substrates using **6** in toluene resulted in the stoichiometric reduction due to subsequent reaction of the borane with the formed alcohols leading to C-B bond cleavage and formation of ether **49**.[129, 130]

Taking a closer look at the deactivation pathway of **6** by water or alcohols under basic conditions, one can conclude that the strength of LB is essential, and irreversible deprotonation of the complexes **6**-H2O or **50** can be

prevented when a weaker LB is used. Consistent with these considerations, two independent studies reported hydrogenation of aldehydes and ketones mediated by **6** in combination with weak ethereal LBs such as Et_2O and 1,4-dioxane.[131, 132] The proposed mechanism is depicted in Fig. 18. Here, H_2 activation occurs between **6** and ethereal solvent (solvent-assisted pathway, Fig. 18, Route A). Being a strong Brønsted acid, protonated ether activates the carbonyl compound followed by hydride transfer from borohydride species to form a borane-alcohol adduct. The latter does not undergo deprotonation with the weak ethereal LB. Since H_2 activation between Et_2O/**6** was demonstrated and employed in hydrogenation catalysis earlier,[133] and taking into the account overwhelming excess of the ethereal donor compared to the carbonyl compound, the substrate assisted pathway was thought to be unlike. (Fig. 18, Route B). It was further shown that **6** remains an active catalyst in the hydrogenation of carbonyl compounds in 1,4-dioxane even in the presence of multiple equivalents of water.[134] Thus, the reaction could be performed in commercial moist solvents in air, albeit under more forcing conditions and longer reaction times.

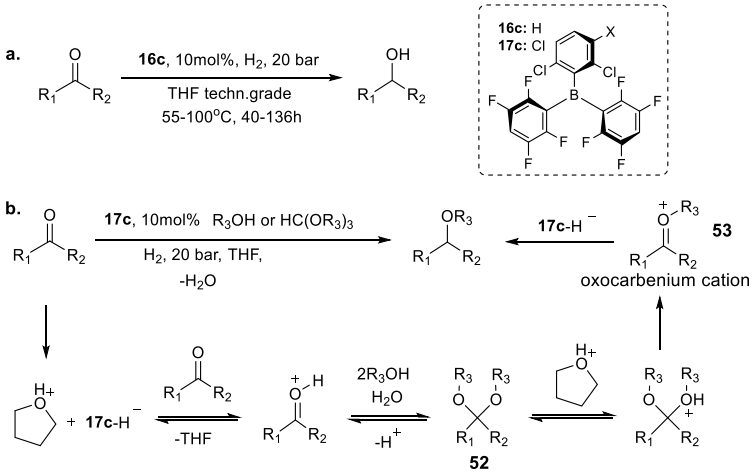

Figure 19 (a) Reduction of carbonyls, and (b) reductive esterification under moist conditions.

Hydrogenation of carbonyl compounds under moist conditions was also independently reported by Soós *et al.* using borane **16c** in technical grade THF (Fig.19, a).[135] In this work, functional group/water tolerance was ensured by weakly basic conditions along with employing a less acidic borane designed according to the size-exclusion principle. As an extension of this work, the same group demonstrated the utility of **17c** in reductive esterification of aldehydes and ketones (Fig.19, b).[136] The sole borane **17c** in THF provided dual function catalysis: Brønsted acid-assisted formation of acetal/ketal **52** followed by FLP-type reduction. Both high H_2O tolerance attributed to the

catalyst and selective reduction of *in situ* formed acetals rather than starting carbonyls are remarkable.

In fact, deprotonation of water adduct **6**-H2O, which occurs in the presence of stronger LBs, was proved to be reversible: hydroxyborate [**6**-OH]$^-$ releases H_2O upon protonation by [HP*t*Bu$_3$]$^+$ - conjugated Brønsted acid of moderate base P*t*Bu$_3$ under forcing conditions.[137] Borane **6** in an amount of just 1 mol% catalysed reductive amination of aldehydes and ketones with anilines using 1.2 equivalents of hydrosilane as a reductant in the presence of up to 100 equivalents of water, derived from imine formation and the use of non-purified solvents (Fig. 20). In the presence of arylamines, boron species exists in catalytically inactive hydroxyborate form [**6**-OH]$^-$. However, heating to 100°C unlocks reprotonation of [**6**-OH]$^-$ to **6**-H2O and further dissociation to release free **6** enough to effect FLP type Si-H bond activation and subsequent reactivity. This methodology could not be applied to more basic alkylamines due to the irreversible deprotonation of **6**-H_2O. Thus, compatibility of **6**/amine pair with H_2O was found to be limited to those amines whose conjugate acids have pKa<16 in MeCN. In the subsequent work, the range of substrates was complemented with alkylamines using less acidic borane BPh_3 (**54**) as a catalyst. In the presence of more basic alkylamines, catalyst is preserved in the form of $AlkNH_2$-**54** and [**54**-OH]$^-$[$AlkNH_3$]$^+$, with weaker aromatic amines equilibrium shifts towards H_2O-**54**, which is prone to deactivation via protodeboronation. Therefore, **54** was only effective for amines whose conjugate acids have pKa>12 in MeCN. Both pathways of catalyst deactivation could be minimized employing moderately Lewis acidic and sterically accessible for coordination of amine borane B(3,5-$Cl_2C_6H_3$)$_3$ (**55**). This catalyst effected reductive amination with a wide range of both aliphatic and aromatic amines corresponding to conjugate acids in the pKa range 10.6-18.5 in MeCN.

Despite notable water tolerance, neither of the aforementioned boranes were capable of reductive amination using H_2 as a reductant under the reported conditions. Presumably, in the case of **6** H_2, activation is kinetically precluded due to the very low concentration of free borane, while boranes **54** and **55** do not reach sufficient cumulative strength in combination with imines/amines presented in the system. This challenge was resolved by Soós *et al.* yet again applying the size-exclusion principle in the borane design. Sterically crowded at boron (2,6-$Cl_2C_6H_3$)$_2$(2-Cl-6-F-C_6H_3) (**56**) in combination with moderately strong and compact base DABCO provided a viable catalyst for reductive amination carbonyls with aryl- and alkylamines and H_2. The system tolerated high contents of water; for instance, 37% aqueous solution of formaldehyde could be used as a reagent. Shortly after Ogoshi et al. reported a similar methodology employing more electrophilic borane **57** as a sole catalyst in the presence of molecular sieves.[138] This work featured impressive substrate scope bearing a wide range of functional groups, including carboxyl, hydroxyl, and additional amino groups (Fig. 21).

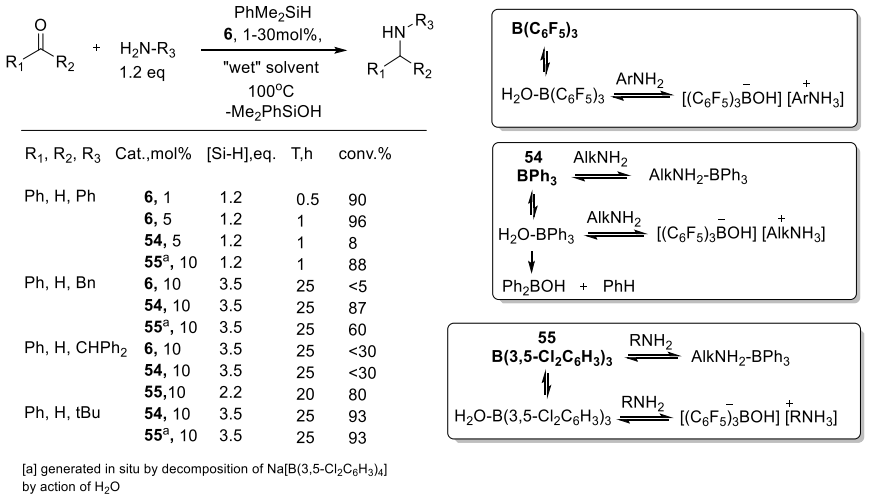

R_1, R_2, R_3	Cat.,mol%	[Si-H],eq.	T,h	conv.%
Ph, H, Ph	**6,** 1	1.2	0.5	90
	6, 5	1.2	1	96
	54, 5	1.2	1	8
	55[a], 10	1.2	1	88
Ph, H, Bn	**6,** 10	3.5	25	<5
	54, 10	3.5	25	87
	55[a], 10	3.5	25	60
Ph, H, $CHPh_2$	**6,** 10	3.5	25	<30
	54, 10	3.5	25	<30
	55,10	2.2	20	80
Ph, H, tBu	**54,** 10	3.5	25	93
	55[a], 10	3.5	25	93

[a] generated in situ by decomposition of $Na[B(3,5\text{-}Cl_2C_6H_3)_4]$ by action of H_2O

Figure 20 Reductive amination of carbonyls with aryl and alkyl amines under "wet" conditions using hydrosilane as a reductant.

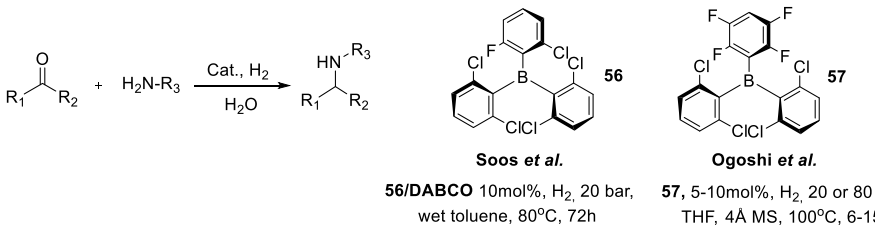

Figure 21 Reductive amination of carbonyls using H_2 as a reductant.

It is also worth noting that there has been growing interest in alternative approach to disfavouring FLPs deactivation by H_2O/O-H bonds by the replacement of B centre into a heavier element to result in a still strong but softer and less oxophilic Lewis acid.[139]

3.4 INTRAMOLECULAR FLPS AMONG OTHERS

As was discussed previously in section 3.1.1, intramolecular systems with spatially close LA and LB centers have the thermodynamic advantage over intermolecular analogs due to larger stabilization interactions ΔG_{stab}. From the kinetic point of view, intramolecular FLPs are somewhat similar to EC and typically feature faster hydrogen addition rates. These features gave grounds to search for superior hydrogenation catalysts among intramolecular systems.

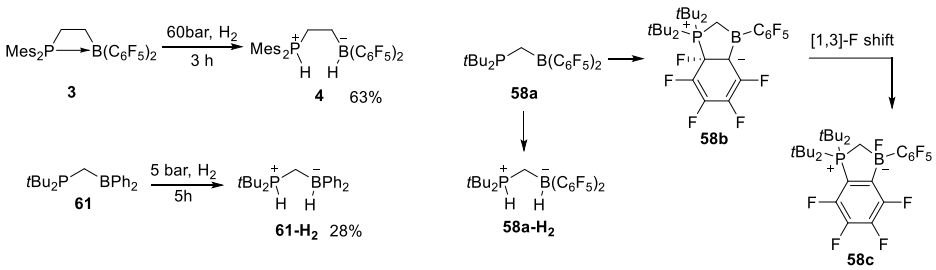

Figure 22 Dihydrogen activation with intramolecular phosphinoboranes.

Phosphonium borate **4** (Fig.22) was shown to be a far more active catalyst in the hydrogenation of imines and enamines than its FLP predecessors. Dihydrogen addition rates to **3** and to its intermolecular analog Mes_3P/**6** are comparable, and so are corresponding activation energies: 21.5 kcal/mol for **3**+H_2[65] compared to 17.7 kcal/mol for Mes_3P /**6**+H_2.[72] Thus, despite **3** having notably less acidic LA site than **6**, it retains high activity towards H_2 likely due to the cooperative effect of the linked system. The following hydrogen transfer step from **4** to the substrate occurs rapidly so that the prior H_2 activation becomes the rate limiting step.[140] Calculated Gibbs free energies of the formation of adducts $[Mes_3PH]^+$[**6**-H]$^-$ and **4** in toluene are -11.6 and −2.4 kcal/mol[51] correspondingly. Naturally, close-to-zero thermodynamics of intermediate **4** favors hydrogen transfer and, therefore, hydrogenation occurs faster. Attempts to obtain phosphinoborane **58a** with shorter methylene linker led to the spontaneous formation of undesirable heterocycle **58c**, which likely proceeds via activation of the *ortho*-C-F bond by the frustrated P/B centres followed by [1,3]-F shift.[141] Surprisingly, **61** bearing simply Ph instead C_6F_5 rings were still capable for H_2 activation under mild conditions.[55] Calculated Gibbs free energies of the formation of hypothetical adduct **58-H₂** and adduct **4** in toluene are -14.8 and -0.7 kcal/mol respectively, whereas activation barriers are 16.6 and 22.6 kcal/mol respectively. These numbers suggest that thermodynamics of H_2 splitting are more sensitive to the electronic effect of LA part than the kinetics and this observation seems to be general for intramolecular systems.[142]

Ansa-aminoborane **22**[101] with substantially more basic TMP group rapidly converts into zwitterionic salt **22-H₂** under 1 atm of H_2 (Fig. 23). Salt **22-H₂** appeared to be air and moisture stable and could be reverted to **22** upon reflux at 110°C in 20 hours. The activation barrier and Gibbs free energy were calculated to be 14.4 kcal/mol[101] and -12 [51] to -7.3 [101] kcal/mol respectively. Combined studies on the structure of **22-H₂** by X-ray and neutron diffraction, DFT calculations, and NOE NMR revealed a strong dihydrogen bond between former H_2 atoms with partially covalent character (1.5-1.8 Å, and 1.78 Å according to X-ray analysis). Such bonding is favorable for facile H_2 release, yet, notable thermodynamic stability of **22-H₂** limited catalyst performance and despite facile H_2 activation the reaction required

prolonged heating (typical conditions: 1 bar H_2, 110°C 6-24 h). Low conversions were observed with sterically accessible and also less basic substrates. With the latter proton transfer seems to become the rate limiting step. In a good agreement with this assumption, further reducing the basicity of amine moiety accelerated H_2 release. For instance, **37-H₂** converts to **37** six times faster and demonstrated substantially improved catalytic activity.

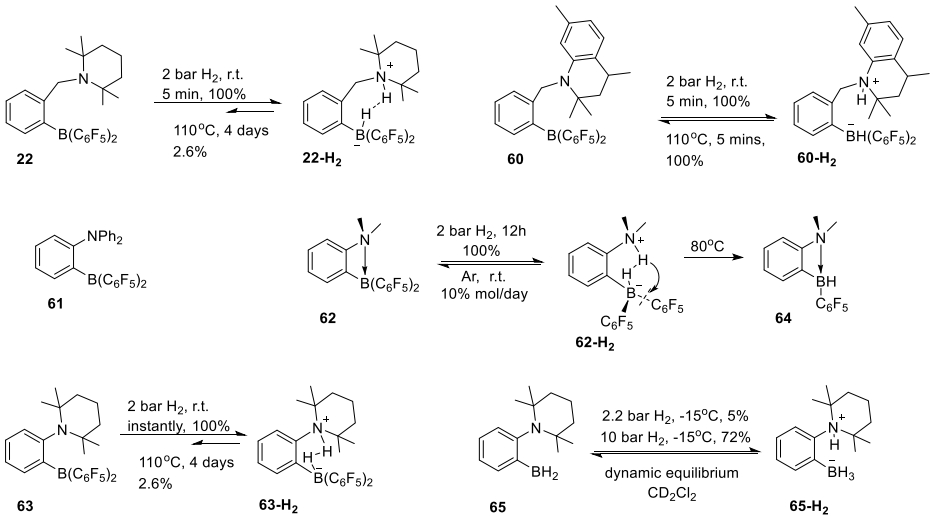

Figure 23 Dihydrogen activation with *ansa*-aminoboranes.

Removal of the methylene linker between the aromatic ring and amine moiety in **22** provides a more rigid *ortho*-phenylene scaffold. In fact, the first example of *ortho*-phenylene templated FLP system **61** was reported by Piers *et al.* a few years before the breakthrough discovery of heterolytic H_2 splitting by the system **1**.[143] Compound **61** formed adducts with acidic molecules HCl and H_2O, yet it failed to activate H_2 due to insufficient basicity of -NPh_2 site. Almost a decade later, our group reported -TMP-and -NMe_2 substituted analogs **62** and **63**, which both readily activated H_2 under mild conditions. [144] Adduct **63-H₂** appeared to be extremely stable not releasing H_2 even upon prolonged heating, presumably due to strong electrostatic stabilization within rigid 6-member ring C-N-H-H-B-C. In contrast, **62** reacted with hydrogen slower but reversibly. Unlike **63,** compound **62** exists as an internal B-N adduct. Since additional energy is required to break B-N bond, H_2 activation is slower than this with **63**. Significant stabilization of the internal adduct **62** is the driving force for the reverse H_2 release. Due to the excessive steric hindrance and thermodynamic stability **63-H₂** could not transfer H_2 to any polar substrates, while **62** effected hydrogenations of sterically accessible substrates. It was noted that upon heating at 80°C adduct **62-H₂** easily

undergoes intramolecular protodeboronation to give *ansa*-aminohydroborane **64**. The latter was found to be an efficient catalyst in the hydrogenation of internal alkynes into *cis*-alkenes. Mechanistic studies revealed that the process occurs via hydroboration of alkyne with **64**, followed by H_2 cleavage and subsequent intramolecular protodeboronation to release alkene and regenerate **64**.[145]

The cooperative effect of phenylene bridged B/N sites appeared to be so powerful that even *ansa*-aminoborane **65** bearing weakly acidic -BH_2 existed in dynamic equilibrium with corresponding adduct **65-H_2** under moderate pressures and temperatures in CD_2Cl_2.[143] Gibbs free energy of -1.1 kcal/mol was obtained from VT ^{1}H NMR study. The kinetic analysis of H_2 release from **65-H_2** using spin-saturation transfer NMR provided free activation energy of 18.3 kcal/mol.

Besides application in catalysis, *ansa*-FLPs have the ability to produce parahydrogen-induced polarization (PHIP). [146] Parahydrogen (pH_2) is one of the spin isomers of molecular hydrogen, in which the two nuclear spins are antiparallel (spin of I = 0). Parahydrogen is NMR silent unless it loses symmetry upon pairwise addition to a catalyst or unsaturated substrate, producing spin polarization well above the thermal level. In the recorded NMR spectra, the signals of the former pH_2 nuclei can exhibit orders of magnitude increased intensities. Thus, the addition of pH_2 to **60** allowed for the detection of NH and BH PHIP signals in the corresponding adduct **60-H_2*** (Fig. 24). PHIP signals disappear upon the nuclei spin relaxation, which results in the observation of just the thermal spectrum. However, since hydrogen uptake by **60** is reversible at elevated temperatures, PHIP signals can be observed as long as pH_2 is supplied to the solution. In contrast, **22** PHIP was only observed after first bubbling due to the irreversible character of the hydrogen uptake.

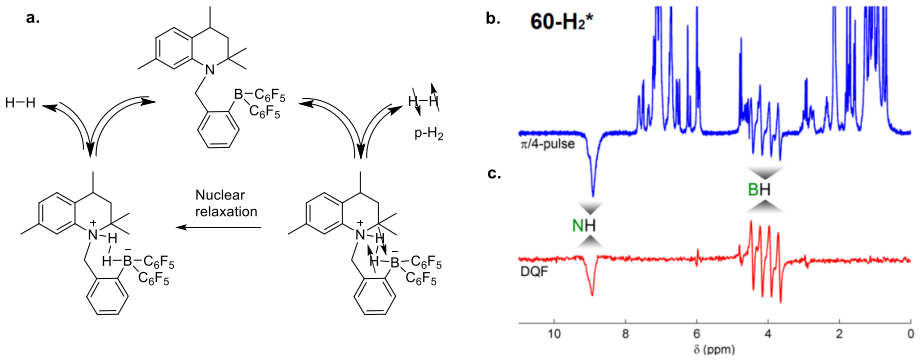

Figure 24 (a) Dynamic chemical equilibrium occurring upon pH_2 bubbling through the solution of **60** at 90°C and corresponding ^{1}H NMR spectra: (b) single shot spectrum, (c) DQF OPSY spectrum.

Certain NMR pulse sequences allow to filter out crowded ^{1}H NMR spectra leaving only PHIP signals. Polarization can also be transferred (spontaneously

or by magnetic field manipulations) to other nuclei, such as ^{13}C and ^{15}N, which are coupled to pH_2-originated protons. These technics are promising for NMR applications, e.g. MRI, since they provide the possibility to enhance signals of compounds in a background-free mode. [146] Apart from NMR/MRI sensitivity boosting, PHIP is useful in mechanistic studies of reactions involving pH_2. Observation of PHIP serves as evidence of pairwise mechanism of H_2 addition/transfer. It also allows to 'light up' trace amounts of intermediate products[147] or coordination compounds.

4 RESULTS AND DISCUSSION

This chapter will briefly cover the results published in publications I-V. More thorough discussions and experimental details can be found in the attached publications and corresponding supplementary materials, which are available free of charge on the publishers' webpages.

4.1 NON-HALOGENATED *ANSA*-AMINOBORANES FOR HIGHLY REVERSIBLE HYDROGEN ACTIVATION [I, II]

The ability of *ansa*-FLPs to produce PHIP is atributable to their unique bifunctional structure, which allows them to fulfill very specific prerequisites:

- Locking pairwise-split H_2 within the H_2 adduct
- Spacious proximity of H_2 originated hydrogens (J-coupling)
- Reversibility of H_2 addition
- High H_2 addition rates

In this work, we aimed to unlock the potential of *ansa*-FLPs as MRI contrasting tags utilizing PHIP. This would require achieving biocompatibility of pH_2 activation process: aqueous media, ambient temperature, and pressure. In the proof-of-principle study, compound **60** enabled continuous production of PHIP only at elevated temperatures, while compound **22** effected PHIP only in the beginning of pH_2 bubbling through the sample due to irreversible formation of the adduct. Besides, both compounds required strictly dry conditions to preserve their reactivity.

We envisioned that phenylene bridged FLPs can provide more favorable parameters for effecting PHIP under ambient conditions: neutral thermodynamics of H_2 addition along with high reaction rates. In such systems, strong electron withdrawing C_6F_5 groups, which are detrimental both in terms of reversibility and moisture sensitivity, can be replaced with substantially less electron withdrawing substituents without sacrificing reactivity towards H_2. Accordingly, we proposed the series of *ansa*-aminoboranes (AABs) represented by the general structure **69** (Fig. 25), where boron is substituted by various non-halogenated aryls (phenyl, 2-isopropylphenyl, mesityl, 2,2-diisopropylphenyl and 2-bisphenyl). Steric hindrance of the aryl substituents was systematically altered with the aim to disfavour B-O bond and, thus, overcome moisture sensitivity.

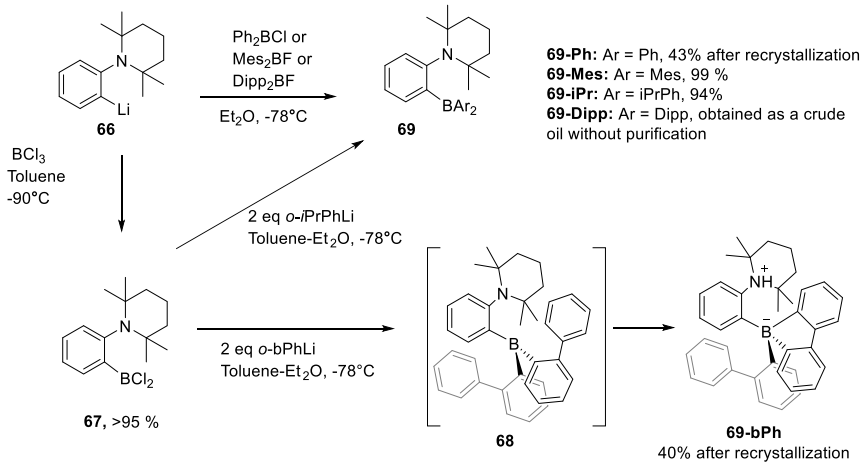

Figure 25 Synthesis of the series of non-halogenated *ansa*-aminoboranes **69**.

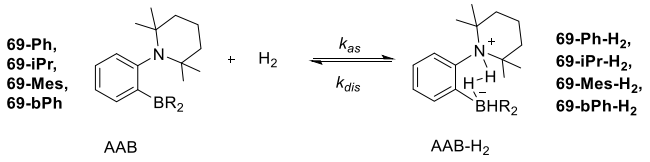

Figure 26 Chemical equilibrium upon H_2 activation with ansa-aminoboranes **69**, except **69-Dipp**, which does not react with hydrogen.

Compounds **69-Ph, 69-Mes** and **69-Dipp** were prepared from the precursor lithium salt **66** and corresponding diarylboron chlorides or fluorides. Due to steric hindrance the reaction between **66** and $Dipp_2BF$ required forcing conditions (60°C, 12 hours) and **69-Dipp** was obtained as crude oil without further purification (see Appendix, A). Compound **69-iPr** was prepared from the salt **66** by one-pot protocol via formation of *ansa*-dichloraminoborane **67** and subsequent addition of 2 equivalents of *ortho*-isopropylphenyl lithium. Intriguingly, treatment of **67** with 2 equivalents of 2-lithiumbiphenyl gave compound **69-bPh** rather than expected bis(2-biphenyl)borylamine **68**, as was confirmed by the single-crystal X-ray diffraction analysis. Compound **69-bPh** is a product of a spontaneous intramolecular C–H insertion of one of the *ortho*-biphenyl substituents attached to the boron atom (reported separately in Publication II).

Hydrogen activation was probed with AABs **69** at room temperature under 10 bars of H_2 in CD_2Cl_2. To our delight, all AABs except the bulkiest **69-Dipp** reacted with H_2 under these conditions. According to ^1H and ^{11}B NMR **69-iPr, -Mes, -bPh** existed in dynamic equilibrium with their adducts with H_2 (Fig. 26), and corresponding conversions are indicated in the Table 1 (column 2). Compound **69-Ph** fully converted to the adduct **69-Ph-H₂** within

10 minutes, however, after the solution was left standing under argon atmosphere for 24 hours it underwent partial dehydrogenation (70% conversion back to **69-Ph**) confirming reversibility of hydrogen uptake at room temperature. Compound **69-Dipp** did not react with H_2 under these conditions, nor H/D scrambling was observed after the solution of **69-Dipp** was left under 5 bars of H_2/D_2 mixture (1:1) for 5 days. ^{1}H NMR of **69-Dipp** revealed that CH protons corresponding to isopropyl groups are non-equivalent and appear as four separate septets, indicating rotational constrains. Along with unfavorable thermodynamics, conformational rigidity might prevent **69-Dipp** to adopt geometry needed for H_2 splitting.

The existence of a dynamic equilibrium between AAB and AAB-H_2 allowed us to determine thermodynamic and kinetic parameters using NMR spectroscopy. Equilibrium constants were determined based on the known initial concentrations of AABs, and ratios of AAB, AAB-H_2 and H_2 signals derived from the integration of ^{1}H NMR signals according to the equation: K_c=[AAB-H_2]/[AAB][H_2]. Additionally, k_{dis} were determined using the spin saturation transfer method upon the reaction with normal H_2. [148,143]

Table 1 *Selected kinetic and thermodynamic parameters for the reactions of AABs **69** with H_2 as determined by NMR spectroscopy.*

AAB	AAB-H_2, % [a]	T (°C)	k_{dis}×10^2(s^{-1})	K_c×10^{-3}(M^{-1})	ΔG
69-Ph	100	0	5.1	7.1	-
		10	38.2	2.1	3.4
		20	160.0	0.9	
		30	540.2	0.3	
69-iPr	90	0	0.2[b]	3.2[c]	-
		10	1.0[b]	1.2[c]	3.2
		20	3.8	0.5	
		30	17.9	0.2	
69-Mes	5	0	0.5[b]	0.014[c]	0
		10	2.2[b]	0.005	
		20	10.4	0.002	
		30	32.2	0.001	
69-bPh	22	-	-	3.0	2.8
69-Dipp	0	-	-	-	-

[a] Measured at RT, 10 bars H_2. [b] Predicted from the Eyring plots using linear regression.

[c] Calculated by extrapolating experimental data

Experiments with pH_2 were conducted with AABs **69-Ph, 69-iPr** and **69-Mes** at various temperatures. Fig. 27a-c shows ^{1}H NMR spectra (^{14}N-decoupled) recorded at 20°C after pH_2 bubbling via PTFE capillary through the 0.05 M AAB solutions for 10 seconds. Antiphase PHIP signals appear for

NH and BH signals. The chart on the Fig. 27 shows combined results for the experiments conducted at various temperatures.

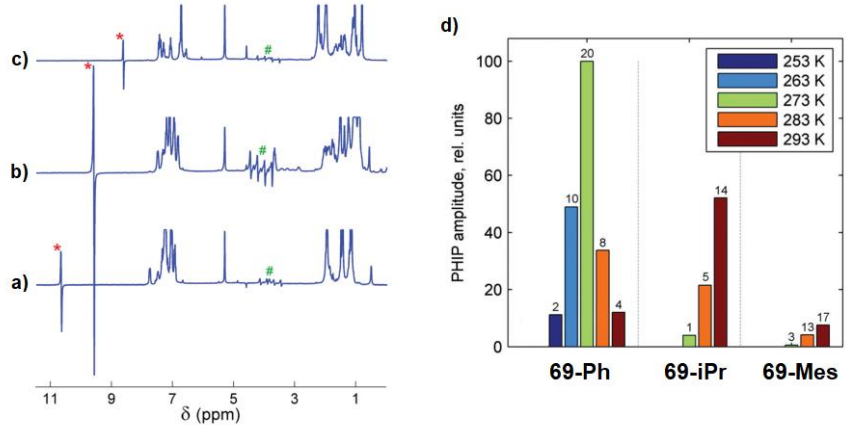

Figure 27 ^{14}N-decoupled ^{1}H NMR spectra acquired at 20°C in the experiments with (a) **69-Ph,** (b) **69-iPr** and (c) **69-Mes**. The antiphase signals of -NH and -BH groups are marked with "*" and "#" correspondingly. (d) Bar chart of PHIP signal amplitudes obtained from the NH proton for the AABs **69-Ph, -iPr, -Mes** (0.05 M solutions) at different temperatures. The numbers above each bar represents the measured signal enhancement factors for these signals.

The amplitude of PHIP signal depends on kinetic and thermodynamic parameters, nuclear relaxation times and $J_{H\text{-}H}$ coupling constants in a rather complex way (Publication I, equation 11). First, it is proportional to AAB's initial concentration, which was the same for all measured samples. Higher $K_c[H_2]_0$ values increase the amplitude by shifting the equilibrium towards higher total concentrations of AAB-H_2, including hyperpolarized AAB–H_2*. Further, nuclear polarization evolves upon the establishment of the chemical equilibrium during pumping of pH_2 into the solution of AAB; on the other hand, nuclear relaxation destroys polarization diminishing PHIP signals. Therefore, fast equilibrium establishment and particularly high k_{dis} (note, addition and dissociation rates are interconnected as $k_{as} = K_c k_{dis}$) allow minimizing negative contribution of the nuclear relaxation. In turn, long relaxation times $^{NH}T_1$ and $^{BH}T_1$ are beneficial for PHIP. Another detrimental factor for PHIP is the mutual cancelation of the antiphase doublets due to line broadening. Accordingly, smaller J_{HH} and shorter $^{NH}T_2$ and $^{BH}T_2$ relaxation times enhance broadening and decrease overall signal intensity. Larger k_{dis} (faster exchange) also enhances the line broadening. One can note that the effect of k_{dis} on the amplitude is dual: when k_{dis} is too low, nuclear relaxation becomes significant, while when k_{dis} is too high, it enhances self-cancellation of the signal. However, the values of k_{dis} at which its negative contribution starts to overrun and cause signal amplitude to decline are well above those

achieved with compounds **69**. Therefore, we can assume this negative contribution is insignificant.

Among all listed parameters, only parameters K_c and k_{dis} varied significantly depending on the chemical structure of **69** and temperature. As can be noted from Table 1, compound **69-Ph** has overall longer (more favorable) K_c and k_{dis} values compared to **69-iPr** and **69-Mes**. Indeed, in the temperature range -20°C to 10°C it shows higher PHIP amplitudes than those observed for **69-iPr** and **69-Mes**. With **69-Ph** PHIP was observed even at sub-zero temperatures in the experiments. Similarly, signal amplitudes achieved with **69-iPr** notably overrun those with **69-Mes**. However, one can note that in the case of **69-iPr** and **69-Mes** PHIP amplitudes increase with temperature, while in the case of **69-Ph** it passes a maximum at 0°C and at 20°C **69-iPr** shows the highest efficiency in the generation of PHIP. Increase of PHIP signal intensity with temperature is expected as k_{dis} grows exponentially. Therefore, abnormal decrease of PHIP signal in the case of **69-Ph** may indicate a competing process of non-pairwise H_2 splitting at higher temperatures. Steric bulk of **69-iPr** and **69-Mes** prevents such possibility.

Despite the hydrophobic and crowded environment around boron, all synthesized AABs reacted with water instantly and irreversibly, except **69-Dipp**, which did not show a sign of reaction or complexation with water. ^{1}H and ^{11}B NMR revealed that the **69-Mes** adduct instantly reacts with water after its solution in toluene being exposed to moist air. The structure of the adduct **69-Mes-H_2O** was confirmed by single-crystal X-ray diffraction analysis.[149] In the solid state **69-Mes-H_2O** features (N)H···O hydrogen bond (1.68(2) Å) , as was also observed in the previously reported adduct **62-H_2O**.[143] Interestingly, B-O and (N)H···O bonds in **69-Mes-H_2O** are only insignificantly elongated compared to those in **62-H_2O**.

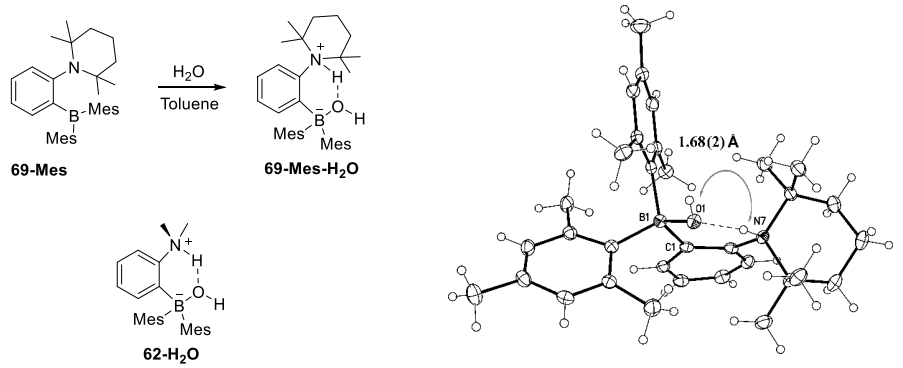

Figure 28 Heterolytic splitting of H_2O by **69-Mes** to give zwitterionic adduct **69-Mes-H_2O**, its X-ray crystal structure, and analogues formation of previously reported **62-H_2O** for comparison. Selected bond lengths (Å) and angles (°): **69-Mes-H_2O:** B-O 1.53(0), (N)H-O 1.68(2), NH 0.93(2), N···O 2.56(9), N-H-O 160; **62-H_2O:** B-O 1.52(1), (N)H-O 1.67, NH 0.93, N···O 2.53(3), N-H-O 152.

4.2 ^{15}N-LABELED *ANSA*-AMINOBORANES FOR PHIP [III]

Compounds **69-Ph, -iPr, and -Mes** generated only modest levels of PHIP signal intensity (20-fold at most). Apart from thermodynamic and kinetic parameters, relaxation times affect the signal amplitudes. In the hyperpolarized adduct AAB-H_2*, both nuclei ^{14}N (I=1) and ^{11}B (I=3/2) to which pH_2 originating protons are attached are quadrupole and have long relaxation times and consequently rapidly quench hyperpolarization. Thus, the replacement of ^{14}N (I=1) with ^{15}N (I=1/2) was expected to affect signal amplitudes. Besides, hyperpolarization can be transferred from the former pH_2 nuclei to the neighbouring heteronuclei such as ^{15}N, ^{13}C, and ^{31}P being observed longer time than on protons (due to the longer relaxation times of heteronuclei compared to protons) The signal of heteronuclei then can be monitored as background free signal, which is of special interest for MRI application. Therefore, we synthesized a series ^{15}N-labeled analog AABs **75-Ph, -Mes, -iPr** according to Fig. 29. Starting from phorone **70** and ^{15}N-ammonium chloride, we synthesized lithium salt **74** in 4 steps. Target AABs **75** were obtained from **74** following the same procedures as described for the non-labeled compounds (Fig. 25).

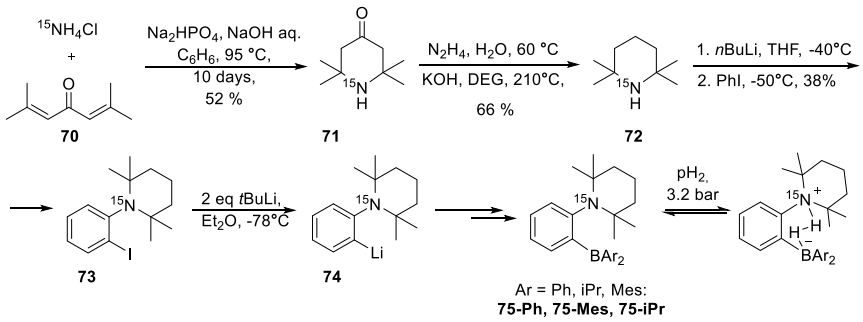

Figure 29 Synthesis of ^{15}N-labeled *ansa*-aminoboranes **75**.

^{1}H NMR experiments recorded after bubbling of pH_2 (91%) through the samples of AABs **75-Ph, -Mes,** and **-iPr** revealed appearance of amplified NH and BH signals with amplitudes comparable to those observed with non-labeled compounds. However, spontaneous hyperpolarization of ^{11}B and ^{15}N nuclei was observed under the same experimental conditions in ^{11}B and ^{15}N NMR spectra. These results are remarkable since rendering hyperpolarization transfer from the former pH_2 nuclei to the neighbouring heteronuclei typically requires modification of the equipment setup or use of sophisticated pulse sequences.[150-152] In the ^{11}B NMR of **75-iPr-H_2**, the BH signal appeared as an antiphase doublet with a 10-fold enhancement compared to the thermal signal. The enhancements for the ^{15}NH signals in the reactions performed at 20 °C were: 150 for **75-Ph**, 350 for **75-iPr**, and 300 for **75-Mes**.

4.3 WATER TOLERANT *ANSA*-PHOSPHINOBORANE [IV]

Compound **69-Mes** appeared to reach a steric threshold in reactivity towards both H_2 and H_2O. Since sterical adjustment at the boron site exceeded its limit, we anticipated that introducing a weaker P-centred Lewis basic site could render H_2O addition notably reversible. To explore this hypothesis, we synthesised *ansa*-phosphinoborane **77** in one step from commercially available materials (Fig. 30). The crystal structure of **77** depicted in Fig. 30 revealed no P-B interaction (P-B distance 3.17(7) Å). To our surprise compound **77** was completely inert towards both H_2 (10 bars) and water at ambient and elevated temperatures.

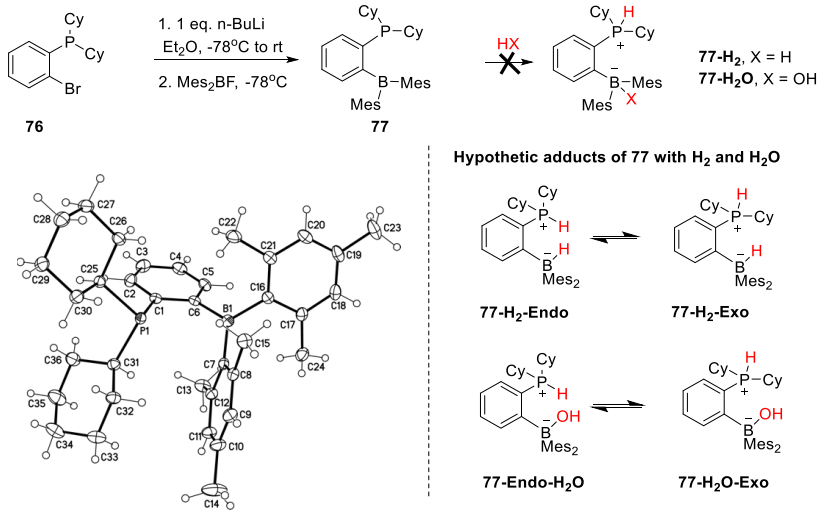

Figure 30 Synthesis of **77** and its X-ray crystal structure; hypothetic adducts of **77** with H_2 and H_2O (*exo*- and *endo*-forms)

Table 2. Calculated Gibbs free energies (kcal/mol) of H_2 and H_2O-adducts with **77**[a]

Adduct	C_6H_6	CH_2Cl_2	MeOH	MeCN
77-H_2-endo	8.0	4.5	3.2	3.0
77-H_2-exo	9.7	6.7	5.4	5.3
77-H_2O-endo	10.0	9.5	10.5	9.1
77-H_2O-exo	5.4	5.5	7.7	5.2

[a] Solution-phase Gibbs free energies for equilibriums **77** + H_2 ⇌ **77-H_2** and **77** + H_2O ⇌ **77-H_2O**

In agreement with experimental observations, DFT calculations showed that formation of adducts **77-H_2** and **77-H_2O** is endergonic (Table 2). For each adduct two isomeric forms were investigated: *endo*, where two ionic fragments of the split molecule are bound (PH···HB or PH···O(H)B), and *exo* without such bonding due to inverted P centre. For H_2 addition in all solvents product

77-H_2-endo appeared to be by about 2 kcal/mol more stable than **77-H_2-exo**, which is promising in light of the importance of H···H bonding for hydrogen release. In contrast, H_2O adduct **77-H_2O-exo** is 3-4 kcal/mol more stable than **77-H_2O-endo**. Previously reported adducts of FLPs with HX molecules typically feature intramolecular bonding H···X (where X=OH, F, Cl)[143, 153, 154], whereas in the case of **77-H_2O** sterics seems to disfavour such corresponding isomer. However, the most inspiring observation was that the addition of H_2 in more polar solvents is more energetically favourable than this of H_2O, confirming that our goal to discriminate these two molecules based on the size is feasible.

4.4 WATER REDUCTION AND HYDROGEN ADDITION IN AQUEOUS CONDITIONS WITH *ANSA*-PHOSPHINOBORANE [VI]

The above experimental and DFT studies on compound **77** encouraged us to explore further *ansa*-phosphinoborane scaffold. To unlock FLP reactivity, we reverted to Lewis acidic site adjustment. Anticipating that the replacement of Me with Cl substituents in *ortho*-positions to B will increase its electron deficiency while retaining the necessary sterics, we synthesised *ansa*-phosphinoborane **80** in three steps depicted in Fig. 31.

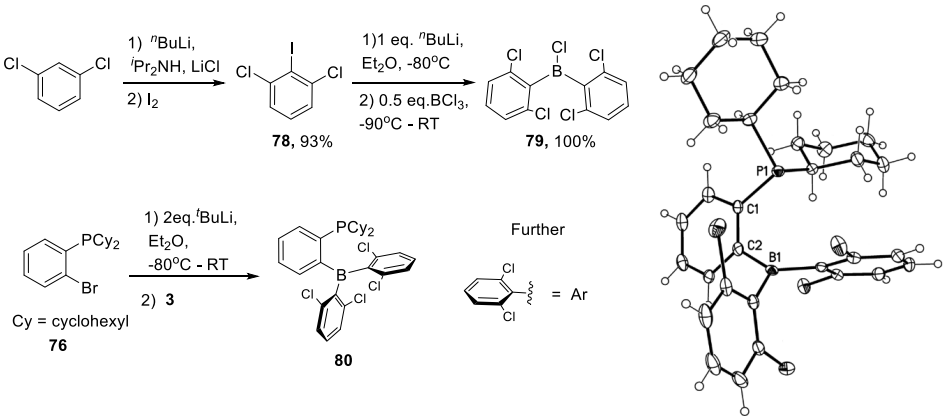

Figure 31 Synthesis of **80** and its X-ray crystal structure.

Upon exposure of **80** to 10 bars of H_2 in CD_2Cl_2, it produced corresponding adduct **80-H_2** quantitatively in 5 minutes; the latter was comprehensively characterized by ^1H and heteronuclear NMR spectroscopy. Isotope scrambling experiments confirmed that H_2 splitting is highly reversible. After the solution of **80-H_2** in C_6D_6 was kept under 5 bars of H_2/D_2 mixture at room temperature for 12 hours, the said gas mixture was converted to HD in ~75%. Water adduct **80-H_2O** rapidly formed upon exposure of **80-H_2** solution to air. Adduct

80-H_2O was prepared separately by reacting **80** with H_2O in CH_2Cl_2 followed by recrystallization. Singal crystal X-ray diffraction showed that in the solid state, **80-H_2O** adopts *exo*-conformation (Fig. 32). Interestingly, it features B-O bond length of 1.46 Å, which is notably shorter than this in *endo*-adducts **62-H_2O** and **69-Mes-H_2O** (1.52 and 1.53 Å respectively).

The observed reactivity of **80** towards H_2 and H_2O was investigated by DFT calculations. In good agreement with the experiments, both H_2 and H_2O addition to **80** were found to be exergonic. The solution Gibbs free energies of formation of **80-H_2O-exo** and **80-H_2O-endo** isomers were calculated to be -3.3 and -1.9 kcal/mol respectively. Intriguingly, calculations showed that the addition of H_2 is more endergonic, predicting energies of **80-H_2-exo** and **80-H_2-endo** to be -5.0 and -6.2 kcal/mol respectively.

In the course of NMR monitoring of **80-H_2O** in the moist mixtures of CD_2Cl_2/CD_3CN we have noted the formation of a new species, accompanied by the appearance of H_2 singlet peak both at room and elevated temperatures. The unknown compound was cleanly produced by heating **80** with 3 equivalents of H_2O in CH_2Cl_2/CH_3CN under inert conditions, isolated, and identified as phosphinoborane oxide **80-O** (Fig.32). Its crystal structure featured B-O-P fragment characterised by B-O and P-O bond lengths of 1.56(9) and 1.55(0) Å respectively.

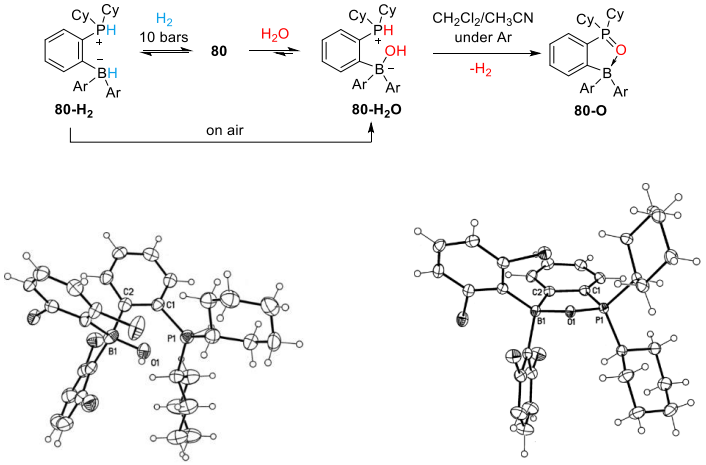

Figure 32 Reactivity of **80** with H_2 and H_2O; X-ray crystal structures of **80-H_2O** (left) and **80-O**(right).

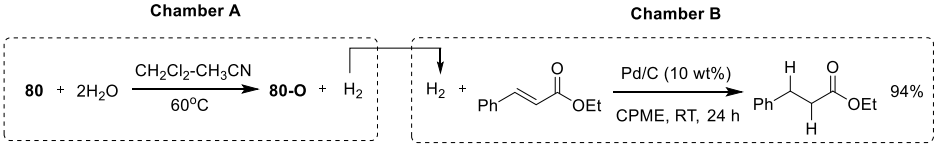

Figure 33 Synthesis of **80** and its X-ray crystal structure.

To confirm that **80** produces an equimolar amount of hydrogen upon the reaction with H_2O we set up the following experiment in the two-chamber reactor: a mixture of **80** and 2 equivalents of H_2O was placed in chamber A to generate H_2, which further reduced ethyl cinnamate (equimolar amount with respect to **80**) placed in the chamber B (Fig. 33).[155] After 24 hours ^1H NMR analysis of the crude product from chamber B revealed close to the quantitative formation of ethyl 3-phenylpropionate.

Indirect reaction between H_2O and R_3P is employed as a source of hydrogen in a number of chemical transformations, such as Mitsunobu reaction or reductive S-S bond cleavage. To the best of our knowledge direct displacement of hydrogen with phosphines from H_2O was not reported so far. The reaction $R_3P + H_2O \rightarrow R_3PO + H_2$ is thermodynamically favorable but kinetically precluded due to the inability of reactants to adopt reasonable configuration to progress towards the products. In fact, geometry distortion can render P(III) center reactive towards polar E-H bonds. This was demonstrated for constrained ONO-supported P(III) complex, which undergoes formal oxidative addition of H_2O to form P(V) complex.[156] Considering other non-metals, examples of H_2O reduction to H_2 are scarce. [41, 157]

To understand the mechanism of H_2O reduction with **80** we carried out kinetic studies employing ^{31}P NMR spectroscopy. The inverse gated proton decoupling pulse sequence ensured quantitative measurements whereas utilization of non-deuterated solvent, namely 1:1 CH_3CN/CH_2Cl_2 mixture, prevented any isotopic exchange side effects. We collected kinetic data at various precise concentrations of H_2O and were surprised to discover that reaction rates are higher at lower concentrations of H_2O. At 65°C the reaction obeys the second order in **1-H_2O** and the reverse first order in H_2O. However, similar experiments carried out at 25 °C revealed first order in **1-H_2O** along with -0.5 order in water. Combined kinetic and computational DFT studies suggested the mechanism depicted in Fig. 34.

In order to reduce computational costs, DFT calculations were performed for the des-chloro analog of **80,** *ansa*-phosphinoborane **81**. Adduct **81-H_2O** exists in rapid equilibrium with the free **81**. The LA center of the latter abstracts water-originated hydrogen atom from the PH in the form of hydride (umpolung of the proton) concurrently with OH migration from the boron to the phosphorus atom. Borohydride **81-H** then reacts with phosphoxonium **81-OH** to give **81-O**, free **81,** and H_2 via proton-hydride recombination. According to the calculations, the hydride abstraction step is rate-determining with the kinetic barrier of 27.5 kcal/mol (in CH_2Cl_2). It involves both water adduct **80-H_2O** and free **80**, giving the first kinetic orders in each of these compounds. Since **80-H_2O** and free **80** exist in rapid equilibrium, the expected kinetic orders 2 in **80-H_2O** and -1 in H_2O are consistent with the ones observed at 65 °C. The alternative unimolecular process featured too high kinetic barrier of 42.5 kcal/mol; besides, it does not conform with the observed kinetics.

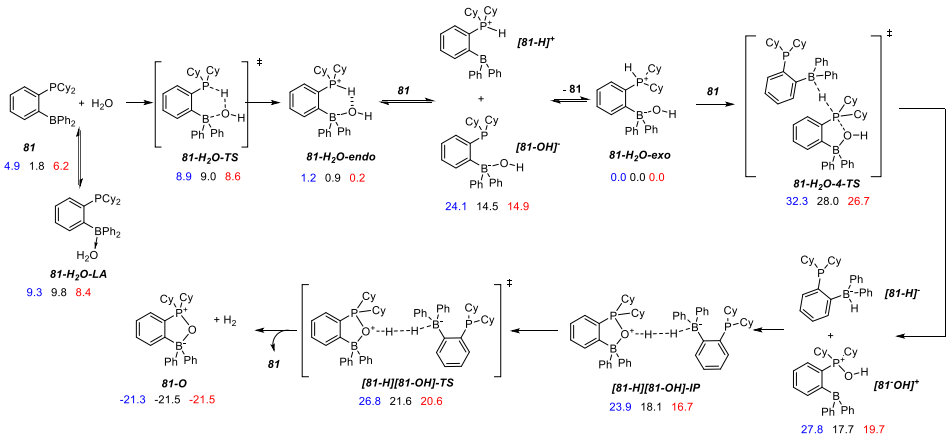

Figure 34 DFT studies of the water reduction mechanism with a model des-chlorophosphinoborane **81**. Solution phase Gibbs free energies computed at the ωB97XD/6-311++G(3df,3pd) level of theory (DFT) are given in kcal/mol with respect to **81-H₂O-exo** in dichloromethane (blue), acetonitrile (black), and water (red).

The results above pointed to the presence of free **8o** in wet solvents. Hence, we could expect to detect formation of **8o-H₂** under such conditions upon addition of H_2. The solution of **8o** in CD_2Cl_2/CD_3CN, containing 6 equivalents of H_2O, was pressurized with 10 bars of H_2 in the gas-tight heavy wall NMR tube and heated at 80°C for an hour, followed by ^1H and heteronuclear NMR analysis. The reaction mixture contained two major species **8o-H₂O** and **8o-O** but also minor species **8o-H₂** (about 13%). Prolonged observation and reliable quantitative monitoring of **8o-H₂** were impossible due to its rapid oxidation and interference of H/D exchange. Similar experiments with pH_2 confirmed the formation of **8o-H₂** by displaying amplified PH and BH PHIP signals. Lower levels of hyperpolarization were observed at ^{31}P and ^{11}B nuclei. The occurrence of PHIP proves that the detected **8o-H₂** is a product of direct H_2 activation by **8o**, rather than an intermediate formed in the course of the reduction of H_2O.

4.5 CATALYTIC ASYMMETRIC HYDROGENATION WITH CAMPHOR-BASED CHIRAL BORANE [V]

When this study was initiated, the highest ees in the FLP-type hydrogenation of imines were obtained with Klankermayer's (1R)-(+)-camphor-based **35a** (up to 83%). This and related reports, however, lacked understanding of the factors governing the enantiocontrol. To address this issue, our collaborators conducted detailed computational DFT studies on the hydrogenation of

PhCMe=NPh **32a** catalysed by **35a**. The reaction was found to be kinetically controlled, and in the stereoselectivity-determining hydride transfer step from borohydride **35a**-H^- to iminium salt **32a**-H^+, several TSs were located within just 5 kcal/mol range. Based on the set of the obtained TSs the enantioselectivity was computed as 80.7%, which is consistent with the experimental ee of 79%. The lowest TS, which leads to the major R enantiomer of **32a** was just 1.5 kcal/mol below the following TS leading to the minor S enantiomer. An essential role in the stabilization of TSs played weak non-covalent interactions, namely π-π stacking, CH_3-π, and Ph-Ph intermolecular contacts. Weak interactions of the Ph group of the catalyst with **32a**-H^+ seemed to be particularly important, and preliminary calculations suggested that introduction substituents at *meta* positions would lead to a greater energetic separation of the two lower transition states, increasing the enantioselectivity.

We were interested to assess the *meta* substituted analogs of **35a** experimentally. We started with a computationally examined candidate, borane **84a**, which was predicted to provide 99.1% ee in the model reaction. Borane **84a** was synthesized following the procedure established for **35a** (Figure 35).[93] Fortunately, separation of diastereoisomers **84a** and **84b** did not require kinetic recrystallization as was described in the said procedure for **35a** and **35b**. Hydroboration of alkene **83** with Piers' borane under solvent-free conditions gave a mixture of **84a** and **84b** in 7:1 ratio. Pure **84a** was isolated from the mixture by simple recrystallization from pentane at -20°C and its structure was confirmed by single crystal X-ray diffraction analysis.

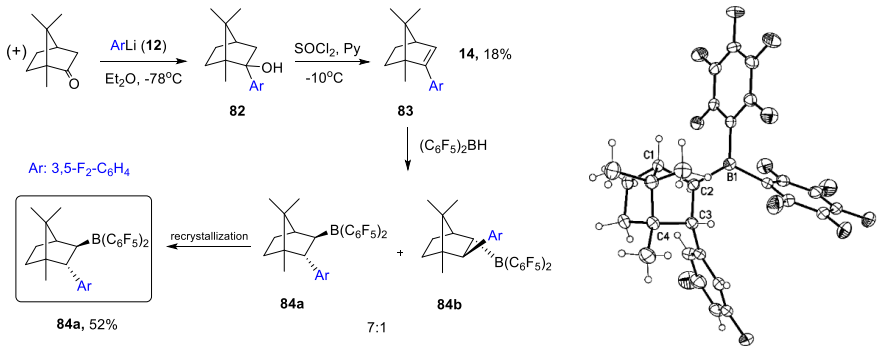

Figure 35 Synthesis of chiral borane **84a** and its X-ray crystal structure.

Unfortunately, catalyst **84a** did not overperform previously reported **35a**, reaching only 75% ee at most in the hydrogenation of the model substrate **32a**, albeit at high conversions. Nevertheless, we decided to investigate another candidate, borane **88** bearing bulky tBu substituents, design of which was guided by chemical intuition. In fact, the most successful chiral FLP catalysts reported

by Du et al. carried substantial steric bulk, which seemed to be a decisive element of the stereocontrol (see section 3.2.2). In the recent report, it was claimed that dispersion interactions rather than steric bulk might be the origin of enantiocontrol with catalyst containing such substituents.[158]

To obtain **88** we developed alternative procedure depicted in Fig. 36, because the addition of 3,5-tBu_2-PhLi or 3,5-tBu_2-PhMgBr to the starting (1R)-(+)-camphor led to its enolization. The last hydroboration step carried out under solvent-free conditions gave exclusively one diastereomer **88** in a quantitative yield. Recrystallization of **88** from n-pentane at -20°C gave crystals suitable for X-ray crystallographic analysis.

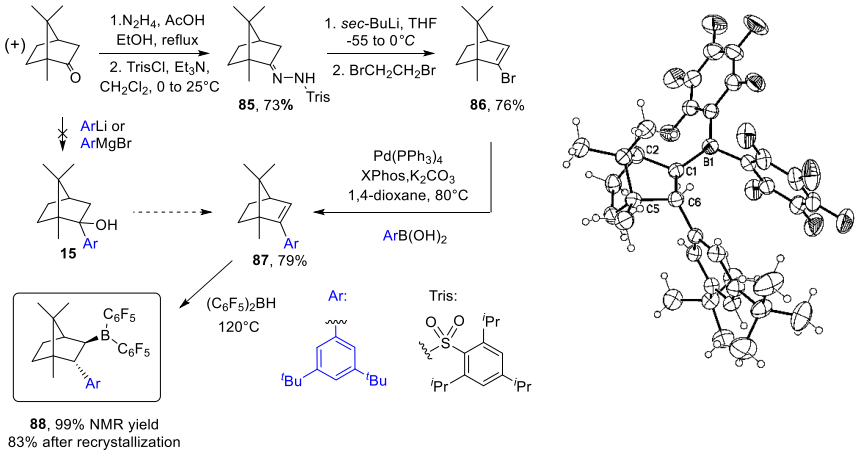

Figure 36 Synthesis of chiral borane **88** and its X-ray crystal structure.

Table 3. Asymmetric hydrogenation of imines with **88**.[a]

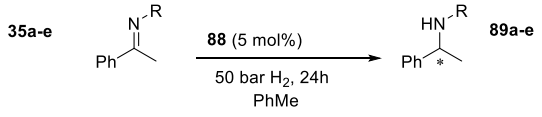

At 25 °C:	Ar = Ph, (**89a**), 99%, 92% ee (*S*) Ar = 4-Me-C_6H_4 (**89b**), 99%, 91% ee (*S*) Ar = 3-Me-C_6H_4 (**89c**), 99%, 93% ee (*S*) Ar = 3,5-Me_2-C_6H_4 (**89d**), 99%, 94% ee (*S*) Ar = 4-MeO-C_6H_4 (**89e**)[b], 99%, 92% ee (*S*)			
		89f 99%, 93% ee (*nd*)	**89g** 99%, 33% ee (*R*)	**89h**[b,c,d] 99%, 21% ee (*S*)
At -15 °C:	**89a**[c] 99%, 95% ee (*S*)	**89d**[c] 99%, 96% ee (*S*)		

[a] Substrate (0.25 mmol), PhMe (0.5ml), conversion by ^{1}H NMR spectroscopy, ee by HPLC (Chiralcel OD-H or OJ-H column). [c] Reaction time 48 h. [d] 10 mol% of **88**

To our delight, when **88** was probed as a catalyst in hydrogenation of model imine **32a** quantitative hydrogenation was observed in 24 hours along with 92% ee. The solvent effect on the stereoselectivity was found to be insignificant. We examined catalyst **88** in the hydrogenation of a small series of imines (Table 3), among which N-aryl-substituted-imines **35b-e** and N-cyclohexyl substituted **35f** gave full conversions and similarly high ees in the range of 91-94%. Enantioselectivity dropped dramatically in the hydrogenation of benzyl-substituted imine **35g** (33% ee). Hydrogenation of quinoline **35h** required higher catalyst loading and prolonged time to achieve the full conversion(10 mol%, 48h) with only 21% ee. Enantioselectivity could be slightly improved upon lowering the temperature to -15°C, as was demonstrated in the hydrogenation of selected imines **35a,d** (95% and 96% ee respectively). As high enantioselectivities in FLP mediated hydrogenation of imines were reported recently by Wang *et al.* utilizing bicyclic borane **43a** at -40°C (up to 95% ee).

5 CONCLUSIONS

Frustrated Lewis pairs exhibit an impressive range of reactivities, yet, just a few were translated into practically valuable processes. One of them, activation of H_2, was employed in hydrogenation catalysis. FLP-type hydrogenation rapidly progressed in terms of substrate scope, functional group tolerance, and selectivity. Besides application in catalysis, intramolecular FLPs have the ability to generate parahydrogen-induced hyperpolarization (PHIP) upon addition of parahydrogen (pH_2). The phenomenon is associated with NMR signal amplification of pH2 derived hydrogens and possibly neighboring nuclei by orders of magnitude. Therefore, linked FLPs have the potential as PHIP contrast agents in NMR and MRI. The reversibility of pH_2 addition and exchange rates are essential for the efficient production of PHIP. To that end, *ortho*-phenylene bridged *(ansa)* FLPs have the advantage of flexibility in terms of strength and sterics of LA and LB sites. This, in turn, ensures high tunability of thermodynamic and kinetic parameters of H_2 addition.

We synthesized the series of *ansa*-aminoboranes **69-Ph**, **-iPr**, **-Mes, -bPh,** and **-Dipp** bearing non-halogenated sterically varying aryls at B site. Reduced acidity of the boryl sites in these compounds allowed to achieve thermodynamically neutral and, consequently, highly reversible H_2 addition at ambient temperatures and pressures. Compound **69-Mes** represented a steric threshold for reactivity, as more hindered **69-Dipp** was inert to H_2 and H_2O. Compound **69-bPh** existed as a zwitterionic adduct formed upon a spontaneous intramolecular splitting of one of the C–H bonds of the *ortho*-biphenyl substituents by B/N centers. This compound was reported as a demonstration of the ability of *ansa*-aminoboranes to activate more challenging sp^2C–H bonds.

Being pressurised with H_2, compounds **69-Ph**, **-iPr**, **-Mes** existed in dynamic chemical equilibrium with the corresponding hydrogen adducts, and respective thermodynamic and kinetic parameters (K_c and k_{dis}) were extracted using NMR spectroscopy. All three compounds provided amplified NH and BH PHIP signals with modest enhancements (up to 20 fold). PHIP could be generated continuously (as long as pH2 was supplied in the solution) at ambient pressures and temperatures, which is optimal in the context of applications. Compound **69-Ph** featured the most suitable characteristics (higher K_c and k_{dis} values) and demonstrated higher levels of PHIP at subzero temperatures. An abnormal decrease in PHIP level was observed at higher temperatures for **69-Ph**, likely indicating switching on non-pairwise activation mode. It was not the case with sterically more bulky **69-iPr** and **69-Mes**, and at room temperature **69-iPr** was found to be the most optimal candidate.

Apart from thermodynamic and kinetic parameters, the NMR properties of the nuclei involved in PHIP, such as relaxation times (T_1 and T_2) are crucial.

Nuclei with longer relaxation times generate stronger PHIP signals with longer observation windows. Introducing ^{15}N nuclei instead of quadrupole ^{14}N within the series **75-Ph**, **-iPr**, **-Mes** led to spontaneous hyperpolarization transfer from p-H_2 derived nuclei to ^{15}N and ^{11}B. PHIP signals of $^{15}NH^+$ exhibited up to 350-fold enhancement.

Despite steric hindrance around B, all compounds except **69-Dipp** reacted with H_2O irreversibly, which means their incompatibility with biological media. In contrast, a structural analog of **69-Mes,** where -TMP is replaced with weaker Lewis basic moiety -PCy_2, *ansa*-phosphinoborane **77** is completely inert towards H_2 and also H_2O. Computational analysis predicted that its hypothetical H_2 adduct is more thermodynamically favorable than the H_2O adduct and suggested that sterics plays the key role in destabilizing the latter.

The above observation encouraged us for further development of the *ansa*-phosphinoborane scaffold. We synthesized **80**, where chlorines in *ortho*-positions to B were intended to unlock FLP reactivity but retain the comparable sterics as its predecessor **77**. Compound **80** activates both H_2 and H_2O in a reversible manner. This allowed detecting adduct **80-H_2** in moist solvents, which was demonstrated in experiments with the thermal polarization and parahydrogen. Compound **80** oxidizes to **80-O** upon unprecedented for phosphines stoichiometric reduction of H_2O to H_2. Combined kinetic and computational studies revealed that the reaction occurs via PH^+ proton umpolung triggered by Lewis acidic site of the free **80**, which exists in rapid equilibrium with **80-H_2O**.

In another part of this work, a modification of previously reported (1R)-(+)-camphor based catalyst **35a**, new chiral borane **88** was synthesized. It was superior to the parental catalyst, giving up to 96% ee in the hydrogenation of imines. Alteration of **35a** leading to **88** was suggested by a computational study carried out by our collaborators and partially by chemical intuition. In addition, unlike **35a,** preparation of **88** did not involve a tedious separation procedure.

In this thesis, thorough structural adjustment guided by complementary theoretical and experimental studies allowed to extend the boundaries of FLPs in a few directions. Firstly, we made a step further towards the practical implementation of FLP mediated PHIP. Secondly, we developed one of the most enantioselective FLP catalyst known to date. However, it was not the rational design, but serendipity, which led us to the discovery of unanticipated stoichiometric reduction of water by one of the studied *ansa*-phosphinoborane. The comprehensive mechanistic study provided a solid basis to further developments in this direction. Certainly, it may help to translate peculiar stoichiometric reactions into catalytically viable processes capable of converting cheap and abundant H_2O into H_2, the substance in greater-than-ever demand.

6 REFERENCES

1. Brown, H. C.; Schlesinger, H. I.; Cardon, S. Z., *J. Am. Chem. Soc.* **1942,** *64* (2), 325-329.
2. Légaré, M.-A.; Courtemanche, M.-A.; Rochette, É.; Fontaine, F.-G., *Science* **2015,** *349* (6247), 513-516.
3. Chernichenko, K.; Lindqvist, M.; Kótai, B.; Nieger, M.; Sorochkina, K.; Pápai, I.; Repo, T., *J. Am. Chem. Soc.* **2016,** *138* (14), 4860-4868.
4. Iashin, V.; Chernichenko, K.; Pápai, I.; Repo, T., *Angew. Chem., Int. Ed.* **2016,** *55* (45), 14146-14150.
5. Dureen, M. A.; Lough, A.; Gilbert, T. M.; Stephan, D. W., *Chem. Commun.* **2008,** (36), 4303-4305.
6. Fan, X.; Zheng, J.; Li, Z. H.; Wang, H., *J. Am. Chem. Soc.* **2015,** *137* (15), 4916-4919.
7. Parks, D. J.; Piers, W. E., *J. Am. Chem. Soc.* **1996,** *118* (39), 9440-9441.
8. Rendler, S.; Oestreich, M., *Angew. Chem., Int. Ed.* **2008,** *47* (32), 5997-6000.
9. Holthausen, M. H.; Bayne, J. M.; Mallov, I.; Dobrovetsky, R.; Stephan, D. W., *J. Am. Chem. Soc.* **2015,** *137* (23), 7298-7301.
10. Caputo, C. B.; Stephan, D. W., *Organometallics* **2012,** *31* (1), 27-30.
11. Mandal, D.; Gupta, R.; Young, R. D., *J. Am. Chem. Soc.* **2018,** *140* (34), 10682-10686.
12. Dureen, M. A.; Welch, G. C.; Gilbert, T. M.; Stephan, D. W., *Inorg. Chem.* **2009,** *48* (20), 9910-9917.
13. Mömming, C. M.; Kehr, G.; Wibbeling, B.; Fröhlich, R.; Erker, G., *Dalton Trans.* **2010,** *39* (32), 7556-7564.
14. Theuergarten, E.; Schlösser, J.; Schlüns, D.; Freytag, M.; Daniliuc, C. G.; Jones, P. G.; Tamm, M., *Dalton Trans.* **2012,** *41* (30), 9101-9110.
15. Mömming, C. M.; Otten, E.; Kehr, G.; Fröhlich, R.; Grimme, S.; Stephan, D. W.; Erker, G., *Angew. Chem., Int. Ed.* **2009,** *48* (36), 6643-6646.
16. Sajid, M.; Klose, A.; Birkmann, B.; Liang, L.; Schirmer, B.; Wiegand, T.; Eckert, H.; Lough, A. J.; Fröhlich, R.; Daniliuc, C. G.; Grimme, S.; Stephan, D. W.; Kehr, G.; Erker, G., *Chem. Sci.* **2013,** *4* (1), 213-219.
17. Otten, E.; Neu, R. C.; Stephan, D. W., *J. Am. Chem. Soc.* **2009,** *131* (29), 9918-9919.
18. Neu, R. C.; Otten, E.; Lough, A.; Stephan, D. W., *Chem. Sci.* **2011,** *2* (1), 170-176.
19. Cardenas, A. J. P.; Culotta, B. J.; Warren, T. H.; Grimme, S.; Stute, A.; Fröhlich, R.; Kehr, G.; Erker, G., *Angew. Chem., Int. Ed.* **2011,** *50* (33), 7567-7571.
20. Sajid, M.; Lawzer, A.; Dong, W.; Rosorius, C.; Sander, W.; Schirmer, B.; Grimme, S.; Daniliuc, C. G.; Kehr, G.; Erker, G., *J. Am. Chem. Soc.* **2013,** *135* (49), 18567-18574.
21. Smirnov, V. O.; Volodin, A. D.; Korlyukov, A. A.; Dilman, A. D., *Angew. Chem., Int. Ed.* **2020,** *59* (30), 12428-12431.

22. Stephan, D. W., Frustrated Lewis Pair Catalysis: An Introduction. In *Frustrated Lewis Pairs*, Chris Slootweg, J.; Jupp, A. R., Eds. Springer International Publishing: Cham, 2021; pp 1-28.
23. Lam, J.; Szkop, K. M.; Mosaferi, E.; Stephan, D. W., *Chem. Soc. Rev.* **2019,** *48* (13), 3592-3612.
24. Spies, P.; Erker, G.; Kehr, G.; Bergander, K.; Fröhlich, R.; Grimme, S.; Stephan, D. W., *Chem. Commun.* **2007,** (47), 5072-5074.
25. Welch, G. C.; Stephan, D. W., *J. Am. Chem. Soc.* **2007,** *129* (7), 1880-1881.
26. Sumerin, V.; Schulz, F.; Nieger, M.; Leskelä, M.; Repo, T.; Rieger, B., *Angew. Chem., Int. Ed.* **2008,** *47* (32), 6001-6003.
27. Chase, P. A.; Welch, G. C.; Jurca, T.; Stephan, D. W., *Angew. Chem., Int. Ed.* **2007,** *46* (42), 8050-8053.
28. Gazis, T. A.; Willcox, D.; Melen, R. L., Lewis Acidic Boranes in Frustrated Lewis Pair Chemistry. In *Frustrated Lewis Pairs*, Chris Slootweg, J.; Jupp, A. R., Eds. Springer International Publishing: Cham, 2021; pp 209-235.
29. Dureen, M. A.; Stephan, D. W., *J. Am. Chem. Soc.* **2009,** *131* (24), 8396-8397.
30. Ménard, G.; Stephan, D. W., *Angew. Chem., Int. Ed.* **2012,** *51* (33), 8272-8275.
31. Xu, M.; Possart, J.; Waked, A. E.; Roy, J.; Uhl, W.; Stephan, D. W., *Philos. Trans. R. Soc. A* **2017,** *375* (2101), 20170014.
32. Backs, J.; Lange, M.; Possart, J.; Wollschläger, A.; Mück-Lichtenfeld, C.; Uhl, W., *Angew. Chem., Int. Ed.* **2017,** *56* (11), 3094-3097.
33. Waerder, B.; Pieper, M.; Körte, L. A.; Kinder, T. A.; Mix, A.; Neumann, B.; Stammler, H.-G.; Mitzel, N. W., *Angew. Chem., Int. Ed.* **2015,** *54* (45), 13416-13419.
34. Scott, D. J.; Phillips, N. A.; Sapsford, J. S.; Deacy, A. C.; Fuchter, M. J.; Ashley, A. E., *Angew. Chem., Int. Ed.* **2016,** *55* (47), 14738-14742.
35. Farrell, J. M.; Hatnean, J. A.; Stephan, D. W., *J. Am. Chem. Soc.* **2012,** *134* (38), 15728-15731.
36. Schäfer, A.; Reißmann, M.; Schäfer, A.; Saak, W.; Haase, D.; Müller, T., *Angew. Chem., Int. Ed.* **2011,** *50* (52), 12636-12638.
37. Schäfer, A.; Reißmann, M.; Schäfer, A.; Schmidtmann, M.; Müller, T., *Chem. – Eur. J.* **2014,** *20* (30), 9381-9386.
38. Clark, E. R.; Ingleson, M. J., *Angew. Chem., Int. Ed.* **2014,** *53* (42), 11306-11309.
39. Chase, P. A.; Stephan, D. W., *Angew. Chem., Int. Ed.* **2008,** *47* (39), 7433-7437.
40. Holschumacher, D.; Bannenberg, T.; Hrib, C. G.; Jones, P. G.; Tamm, M., *Angew. Chem., Int. Ed.* **2008,** *47* (39), 7428-7432.
41. Mo, Z.; Szilvási, T.; Zhou, Y.-P.; Yao, S.; Driess, M., *Angew. Chem., Int. Ed.* **2017,** *56* (13), 3699-3702.
42. Xu, X.; Kehr, G.; Daniliuc, C. G.; Erker, G., *J. Am. Chem. Soc.* **2013,** *135* (17), 6465-6476.
43. Hidalgo, N.; Alférez, M. G.; Campos, J., Frustrated Lewis Pairs Based on Transition Metals. In *Frustrated Lewis Pairs*, Chris Slootweg, J.; Jupp, A. R., Eds. Springer International Publishing: Cham, 2021; pp 319-359.

44. Johnstone, T. C.; Wee, G. N. J. H.; Stephan, D. W., *Angew. Chem., Int. Ed.* **2018,** *57* (20), 5881-5884.
45. Hoshimoto, Y.; Kinoshita, T.; Ohashi, M.; Ogoshi, S., *Angew. Chem., Int. Ed.* **2015,** *54* (40), 11666-11671.
46. Fan, L.; Jupp, A. R.; Stephan, D. W., *J. Am. Chem. Soc.* **2018,** *140* (26), 8119-8123.
47. Liu, L.; Cao, L. L.; Shao, Y.; Ménard, G.; Stephan, D. W., *Chem* **2017,** *3* (2), 259-267.
48. Aramaki, Y.; Imaizumi, N.; Hotta, M.; Kumagai, J.; Ooi, T., *Chem. Sci.* **2020,** *11* (17), 4305-4311.
49. Soltani, Y.; Dasgupta, A.; Gazis, T. A.; Ould, D. M. C.; Richards, E.; Slater, B.; Stefkova, K.; Vladimirov, V. Y.; Wilkins, L. C.; Willcox, D.; Melen, R. L., *Cell Rep.* **2020,** *1* (2), 100016.
50. Holtrop, F.; Jupp, A. R.; Chris Slootweg, J., Radicals in Frustrated Lewis Pair Chemistry. In *Frustrated Lewis Pairs*, Chris Slootweg, J.; Jupp, A. R., Eds. Springer International Publishing: Cham, 2021; pp 361-385.
51. Rokob, T. A.; Hamza, A.; Pápai, I., *J. Am. Chem. Soc.* **2009,** *131* (30), 10701-10710.
52. Rokob, T. A.; Pápai, I., Hydrogen Activation by Frustrated Lewis Pairs: Insights from Computational Studies. In *Frustrated Lewis Pairs I: Uncovering and Understanding*, Erker, G.; Stephan, D. W., Eds. Springer Berlin Heidelberg: Berlin, Heidelberg, 2013; pp 157-211.
53. Pyykkö, P.; Wang, C., *Phys. Chem. Chem. Phys.* **2010,** *12* (1), 149-155.
54. Dorkó, É.; Kótai, B.; Földes, T.; Gyömöre, Á.; Pápai, I.; Soós, T., *J. Organomet. Chem.* **2017,** *847*, 258-262.
55. Bertini, F.; Lyaskovskyy, V.; Timmer, B. J. J.; de Kanter, F. J. J.; Lutz, M.; Ehlers, A. W.; Slootweg, J. C.; Lammertsma, K., *J. Am. Chem. Soc.* **2012,** *134* (1), 201-204.
56. Tague, T. J.; Andrews, L., *J. Am. Chem. Soc.* **1994,** *116* (11), 4970-4976.
57. Moroz, A.; Sweany, R. L.; Whittenburg, S. L., *J. Phys. Chem.* **1990,** *94* (4), 1352-1357.
58. Fan, C.; Mercier, L. G.; Piers, W. E.; Tuononen, H. M.; Parvez, M., *J. Am. Chem. Soc.* **2010,** *132* (28), 9604-9606.
59. Houghton, A. Y.; Karttunen, V. A.; Fan, C.; Piers, W. E.; Tuononen, H. M., *J. Am. Chem. Soc.* **2013,** *135* (2), 941-947.
60. Lu, Z.; Cheng, Z.; Chen, Z.; Weng, L.; Li, Z. H.; Wang, H., *Angew. Chem., Int. Ed.* **2011,** *50* (51), 12227-12231.
61. Nikonov, G. I.; Vyboishchikov, S. F.; Shirobokov, O. G., *J. Am. Chem. Soc.* **2012,** *134* (12), 5488-5491.
62. Rokob, T. A.; Hamza, A.; Stirling, A.; Soós, T.; Pápai, I., *Angew. Chem., Int. Ed.* **2008,** *47* (13), 2435-2438.
63. Kim, H. W.; Rhee, Y. M., *Chem. – Eur. J.* **2009,** *15* (48), 13348-13355.
64. Hamza, A.; Stirling, A.; András Rokob, T.; Pápai, I., *Int. J. Quantum Chem.* **2009,** *109* (11), 2416-2425.
65. Grimme, S.; Kruse, H.; Goerigk, L.; Erker, G., *Angew. Chem., Int. Ed.* **2010,** *49* (8), 1402-1405.
66. Rokob, T. A.; Bakó, I.; Stirling, A.; Hamza, A.; Pápai, I., *J. Am. Chem. Soc.* **2013,** *135* (11), 4425-4437.
67. Bakó, I.; Stirling, A.; Bálint, S.; Pápai, I., *Dalton Trans.* **2012,** *41* (30), 9023-9025.

68. Pu, M.; Privalov, T., *Isr. J. Chem.* **2015,** *55* (2), 179-195.
69. Dang, L. X.; Schenter, G. K.; Chang, T.-M.; Kathmann, S. M.; Autrey, T., *J. Phys. Chem. Letters* **2012,** *3* (22), 3312-3319.
70. Brown, L. C.; Hogg, J. M.; Gilmore, M.; Moura, L.; Imberti, S.; Gärtner, S.; Gunaratne, H. Q. N.; O'Donnell, R. J.; Artioli, N.; Holbrey, J. D.; Swadźba-Kwaśny, M., *Chem. Commun.* **2018,** *54* (63), 8689-8692.
71. Rocchigiani, L.; Ciancaleoni, G.; Zuccaccia, C.; Macchioni, A., *J. Am. Chem. Soc.* **2014,** *136* (1), 112-115.
72. Houghton, A. Y.; Autrey, T., *J. Phys. Chem. A* **2017,** *121* (46), 8785-8790.
73. Mayer, U.; Gutmann, V.; Gerger, W., *Monatshefte für Chemie / Chemical Monthly* **1975,** *106* (6), 1235-1257.
74. Beckett, M. A.; Strickland, G. C.; Holland, J. R.; Sukumar Varma, K., *Polymer* **1996,** *37* (20), 4629-4631.
75. Childs, R. F.; Mulholland, D. L.; Nixon, A., *Can. J. Chem.* **1982,** *60* (6), 801-808.
76. Mock, M. T.; Potter, R. G.; Camaioni, D. M.; Li, J.; Dougherty, W. G.; Kassel, W. S.; Twamley, B.; DuBois, D. L., *J. Am. Chem. Soc.* **2009,** *131* (40), 14454-14465.
77. Christe, K. O.; Dixon, D. A.; McLemore, D.; Wilson, W. W.; Sheehy, J. A.; Boatz, J. A., *J. Fluor. Chem.* **2000,** *101* (2), 151-153.
78. Cummings, S. A.; Iimura, M.; Harlan, C. J.; Kwaan, R. J.; Trieu, I. V.; Norton, J. R.; Bridgewater, B. M.; Jäkle, F.; Sundararaman, A.; Tilset, M., *Organometallics* **2006,** *25* (7), 1565-1568.
79. Ashley, A. E.; Herrington, T. J.; Wildgoose, G. G.; Zaher, H.; Thompson, A. L.; Rees, N. H.; Krämer, T.; O'Hare, D., *J. Am. Chem. Soc.* **2011,** *133* (37), 14727-14740.
80. Parr, R. G.; Szentpály, L. v.; Liu, S., *J. Am. Chem. Soc.* **1999,** *121* (9), 1922-1924.
81. Jupp, A. R.; Johnstone, T. C.; Stephan, D. W., *Dalton Trans.* **2018,** *47* (20), 7029-7035.
82. Lawson, J. R.; Wilkins, L. C.; Melen, R. L., *Chem. – Eur. J.* **2017,** *23* (46), 10997-11000.
83. Ullrich, M.; Lough, A. J.; Stephan, D. W., *J. Am. Chem. Soc.* **2009,** *131* (1), 52-53.
84. Greb, L.; Daniliuc, C.-G.; Bergander, K.; Paradies, J., *Angew. Chem., Int. Ed.* **2013,** *52* (22), 5876-5879.
85. Nicasio, J. A.; Steinberg, S.; Inés, B.; Alcarazo, M., *Chem. – Eur. J.* **2013,** *19* (33), 11016-11020.
86. Keess, S.; Simonneau, A.; Oestreich, M., *Organometallics* **2015,** *34* (4), 790-799.
87. Stepen, A. J.; Bursch, M.; Grimme, S.; Stephan, D. W.; Paradies, J., *Angew. Chem., Int. Ed.* **2018,** *57* (46), 15253-15256.
88. Khan, I.; Manzotti, M.; Tizzard, G. J.; Coles, S. J.; Melen, R. L.; Morrill, L. C., *ACS Catal.* **2017,** *7* (11), 7748-7752.
89. Heshmat, M.; Ensing, B., *J. Phys. Chem. A* **2020,** *124* (32), 6399-6410.
90. Körte, L. A.; Schwabedissen, J.; Soffner, M.; Blomeyer, S.; Reuter, C. G.; Vishnevskiy, Y. V.; Neumann, B.; Stammler, H.-G.; Mitzel, N. W., *Angew. Chem., Int. Ed.* **2017,** *56* (29), 8578-8582.

91. Ben Saida, A.; Chardon, A.; Osi, A.; Tumanov, N.; Wouters, J.; Adjieufack, A. I.; Champagne, B.; Berionni, G., *Angew. Chem., Int. Ed.* **2019,** *58* (47), 16889-16893.
92. Chase, P. A.; Jurca, T.; Stephan, D. W., *Chem. Commun.* **2008,** (14), 1701-1703.
93. Chen, D.; Klankermayer, J., *Chem. Commun.* **2008,** (18), 2130-2131.
94. Geier, S. J.; Chase, P. A.; Stephan, D. W., *Chem. Commun.* **2010,** *46* (27), 4884-4886.
95. Stephan, D. W.; Greenberg, S.; Graham, T. W.; Chase, P.; Hastie, J. J.; Geier, S. J.; Farrell, J. M.; Brown, C. C.; Heiden, Z. M.; Welch, G. C.; Ullrich, M., *Inorg. Chem.* **2011,** *50* (24), 12338-12348.
96. Tussing, S.; Greb, L.; Tamke, S.; Schirmer, B.; Muhle-Goll, C.; Luy, B.; Paradies, J., *Chem. – Eur. J.***2015,** *21* (22), 8056-8059.
97. Tussing, S.; Kaupmees, K.; Paradies, J., *Chem. – Eur. J.* **2016,** *22* (22), 7422-7426.
98. Erős, G.; Nagy, K.; Mehdi, H.; Pápai, I.; Nagy, P.; Király, P.; Tárkányi, G.; Soós, T., *Chem. – Eur. J.* **2012,** *18* (2), 574-585.
99. Erős, G.; Mehdi, H.; Pápai, I.; Rokob, T. A.; Király, P.; Tárkányi, G.; Soós, T., *Angew. Chem., Int. Ed.* **2010,** *49* (37), 6559-6563.
100. Spies, P.; Schwendemann, S.; Lange, S.; Kehr, G.; Fröhlich, R.; Erker, G., *Angew. Chem., Int. Ed.* **2008,** *47* (39), 7543-7546.
101. Sumerin, V.; Schulz, F.; Atsumi, M.; Wang, C.; Nieger, M.; Leskelä, M.; Repo, T.; Pyykkö, P.; Rieger, B., *J. Am. Chem. Soc.* **2008,** *130* (43), 14117-14119.
102. Elmer, L.-M.; Kehr, G.; Daniliuc, C. G.; Siedow, M.; Eckert, H.; Tesch, M.; Studer, A.; Williams, K.; Warren, T. H.; Erker, G., *Chem. – Eur. J.* **2017,** *23* (25), 6056-6068.
103. Özgün, T.; Ye, K.-Y.; Daniliuc, C. G.; Wibbeling, B.; Liu, L.; Grimme, S.; Kehr, G.; Erker, G., *Chem. – Eur. J.***2016,** *22* (17), 5988-5995.
104. Wang, X.; Kehr, G.; Daniliuc, C. G.; Erker, G., *J. Am. Chem. Soc.* **2014,** *136* (8), 3293-3303.
105. Jian, Z.; Kehr, G.; Daniliuc, C. G.; Wibbeling, B.; Erker, G., *Dalton Trans.* **2017,** *46* (35), 11715-11721.
106. Jian, Z.; Krupski, S.; Škoch, K.; Kehr, G.; Daniliuc, C. G.; Císařová, I.; Štěpnička, P.; Erker, G., *Organometallics* **2017,** *36* (15), 2940-2946.
107. Wang, H.; Fröhlich, R.; Kehr, G.; Erker, G., *Chem. Commun.* **2008,** (45), 5966-5968.
108. Greb, L.; Oña-Burgos, P.; Kubas, A.; Falk, F. C.; Breher, F.; Fink, K.; Paradies, J., *Dalton Trans.* **2012,** *41* (30), 9056-9060.
109. Scott, D. J.; Fuchter, M. J.; Ashley, A. E., *Angew. Chem., Int. Ed.* **2014,** *53* (38), 10218-10222.
110. Lam, J.; Günther, B. A. R.; Farrell, J. M.; Eisenberger, P.; Bestvater, B. P.; Newman, P. D.; Melen, R. L.; Crudden, C. M.; Stephan, D. W., *Dalton Trans.* **2016,** *45* (39), 15303-15316.
111. Aupic, C.; Abdou Mohamed, A.; Figliola, C.; Nava, P.; Tuccio, B.; Chouraqui, G.; Parrain, J.-L.; Chuzel, O., *Chem. Sci.* **2019,** *10* (26), 6524-6530.
112. Ghattas, G.; Chen, D.; Pan, F.; Klankermayer, J., *Dalton Trans.* **2012,** *41* (30), 9026-9028.

113. Sumerin, V.; Chernichenko, K.; Nieger, M.; Leskelä, M.; Rieger, B.; Repo, T., *Adv. Synth. Catal.* **2011,** *353* (11-12), 2093-2110.
114. Lindqvist, M.; Borre, K.; Axenov, K.; Kótai, B.; Nieger, M.; Leskelä, M.; Pápai, I.; Repo, T., *J. Am. Chem. Soc.* **2015,** *137* (12), 4038-4041.
115. Meng, W.; Feng, X.; Du, H., *Acc. Chem. Res.* **2018,** *51* (1), 191-201.
116. Liu, Y.; Du, H., *J. Am. Chem. Soc.* **2013,** *135* (18), 6810-6813.
117. Zhang, Z.; Du, H., *Angew. Chem., Int. Ed.* **2015,** *54* (2), 623-626.
118. Zhang, Z.; Du, H., *Organic Letters* **2015,** *17* (11), 2816-2819.
119. Zhang, Z.; Du, H., *Organic Letters* **2015,** *17* (24), 6266-6269.
120. Feng, X.; Meng, W.; Du, H., Frustrated Lewis Pair Catalyzed Asymmetric Reactions. In *Frustrated Lewis Pairs*, Chris Slootweg, J.; Jupp, A. R., Eds. Springer International Publishing: Cham, 2021; pp 29-86.
121. Wei, S.; Du, H., *J. Am. Chem. Soc.* **2014,** *136* (35), 12261-12264.
122. Tu, X.-S.; Zeng, N.-N.; Li, R.-Y.; Zhao, Y.-Q.; Xie, D.-Z.; Peng, Q.; Wang, X.-C., *Angew. Chem., Int. Ed.* **2018,** *57* (46), 15096-15100.
123. Gao, B.; Feng, X.; Meng, W.; Du, H., *Angew. Chem., Int. Ed.* **2020,** *59* (11), 4498-4504.
124. Piers, W. E.; Chivers, T., *Chem. Soc. Rev.* **1997,** *26* (5), 345-354.
125. Erker, G., *Dalton Trans.* **2005,** (11), 1883-1890.
126. Bergquist, C.; Bridgewater, B. M.; Harlan, C. J.; Norton, J. R.; Friesner, R. A.; Parkin, G., *J. Am. Chem. Soc.* **2000,** *122* (43), 10581-10590.
127. Dong, Y.; Zhang, H.; Yang, J.; He, S.; Shi, Z.-C.; Zhang, X.-M.; Wang, J.-Y., *ACS Omega* **2019,** *4* (25), 21567-21577.
128. Nyhlén, J.; Privalov, T., *Dalton Trans.* **2009,** (29), 5780-5786.
129. Longobardi, L. E.; Tang, C.; Stephan, D. W., *Dalton Trans.* **2014,** *43* (42), 15723-15726.
130. Lindqvist, M.; Sarnela, N.; Sumerin, V.; Chernichenko, K.; Leskelä, M.; Repo, T., *Dalton Trans.* **2012,** *41* (15), 4310-4312.
131. Mahdi, T.; Stephan, D. W., *J. Am. Chem. Soc.* **2014,** *136* (45), 15809-15812.
132. Scott, D.; Fuchter, M.; Ashley, A., *J. Am. Chem. Soc.* **2014,** *136*.
133. Hounjet, L. J.; Bannwarth, C.; Garon, C. N.; Caputo, C. B.; Grimme, S.; Stephan, D. W., *Angew. Chem., Int. Ed.* **2013,** *52* (29), 7492-7495.
134. Scott, D. J.; Simmons, T. R.; Lawrence, E. J.; Wildgoose, G. G.; Fuchter, M. J.; Ashley, A. E., *ACS Catal.* **2015,** *5* (9), 5540-5544.
135. Gyömöre, Á.; Bakos, M.; Földes, T.; Pápai, I.; Domján, A.; Soós, T ., *ACS Catal.* **2015,** *5* (9), 5366-5372.
136. Bakos, M.; Gyömöre, Á.; Domján, A.; Soós, T., *Angew. Chem., Int. Ed.* **2017,** *56* (19), 5217-5221.
137. Ghattas, G.; Bizzarri, C.; Hölscher, M.; Langanke, J.; Gürtler, C.; Leitner, W.; Subhani, M. A., *Chem. Commun.* **2017,** *53* (22), 3205-3208.
138. Hoshimoto, Y.; Kinoshita, T.; Hazra, S.; Ohashi, M.; Ogoshi, S., *J. Am. Chem. Soc.* **2018,** *140* (23), 7292-7300.
139. Fasano, V.; Ingleson, M. J., *Synthesis* **2018,** *50* (09), 1783-1795.
140. Whittemore, S. M.; Edvenson, G.; Camaioni, D. M.; Karkamkar, A.; Neiner, D.; Parab, K.; Autrey, T., *Catal. Today* **2015,** *251*, 28-33.
141. Zhao, X.; Gilbert, T. M.; Stephan, D. W., *Chem. – Eur. J.* **2010,** *16* (34), 10304-10308.
142. Zhang, J.; Shao, Y.; Li, Y.; Liu, Y.; Ke, Z., *Chin. Chem. Lett.* **2018,** *29* (8), 1226-1232.

143. Roesler, R.; Piers, W. E.; Parvez, M., *J. Organomet. Chem.* **2003,** *680* (1), 218-222.
144. Chernichenko, K.; Nieger, M.; Leskelä, M.; Repo, T., *Dalton Trans.* **2012,** *41* (30), 9029-9032.
145. Chernichenko, K.; Madarász, Á.; Pápai, I.; Nieger, M.; Leskelä, M.; Repo, T., *Nat. Chem.* **2013,** *5* (8), 718-723.
146. Natterer, J.; Bargon, J., *Prog. Nucl. Magn. Reson. Spectrosc.* **1997,** *31* (4), 293-315.
147. Duckett, S. B.; Newell, C. L.; Eisenberg, R., *J. Am. Chem. Soc.* **1994,** *116* (23), 10548-10556.
148. Jarek, R. L.; Flesher, R. J.; Shin, S. K., *J. Chem. Educ.* **1997,** *74* (8), 978.
149. Nieger, M.; Sorochkina, K.; Chernichenko, K.; Repo, T., CCDC 2121061: Experimental Crystal Structure Determination, **2021**, DOI: 10.5517/ccdc.csd.cc2964b0
150. Theis, T.; Truong, M. L.; Coffey, A. M.; Shchepin, R. V.; Waddell, K. W.; Shi, F.; Goodson, B. M.; Warren, W. S.; Chekmenev, E. Y., *J. Am. Chem. Soc.* **2015,** *137* (4), 1404-1407.
151. Golman, K.; Axelsson, O.; Jóhannesson, H.; Månsson, S.; Olofsson, C.; Petersson, J. S., Magn. Reson. Med. **2001,** *46* (1), 1-5.
152. Kuhn, L. T.; Bargon, J., Transfer of Parahydrogen-Induced Hyperpolarization to Heteronuclei. In *In situ NMR Methods in Catalysis*, Bargon, J.; Kuhn, L. T., Eds. Springer Berlin Heidelberg: Berlin, Heidelberg, 2007; pp 25-68.
153. Moebs-Sanchez, S.; Saffon, N.; Bouhadir, G.; Maron, L.; Bourissou, D., *Dalton Trans.* **2010,** *39* (18), 4417-4420.
154. Chernichenko, K.; Kótai, B.; Nieger, M.; Heikkinen, S.; Pápai, I.; Repo, T., *Dalton Trans.* **2017,** *46* (7), 2263-2269.
155. Friis, S. D.; Lindhardt, A. T.; Skrydstrup, T., *Acc. Chem. Res.* **2016,** *49* (4), 594-605.
156. Robinson, T. P.; De Rosa, D. M.; Aldridge, S.; Goicoechea, J. M., *Angew. Chem., Int. Ed.* **2015,** *54* (46), 13758-13763.
157. Flinker, M.; Yin, H.; Juhl, R. W.; Eikeland, E. Z.; Overgaard, J.; Nielsen, D. U.; Skrydstrup, T., *Angew. Chem., Int. Ed.* **2017,** *56* (50), 15910-15915.
158. Eschmann, C.; Song, L.; Schreiner, P. R., *Angew. Chem., Int. Ed.* **2021,** *60* (9), 4823-4832.

7 APPENDIX

A. Preparation of 69-Dipp

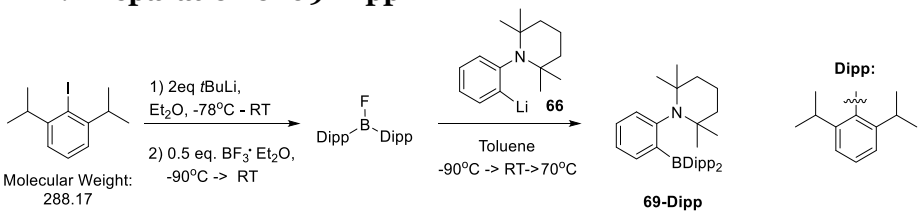

Starting material 2-iodo-1,3-diisopropylbenzene was synthesized from 2,6-diisopropylaniline according to the reported procedure (Bolstad, D. B. *et al.*, *J. Med. Chem.* 2008, *51*, 6839-6852). At - 78°C, *tert*-butyllithium (2.82 ml of 1.7 M solution in hexane, 4.8 mmol) was added dropwise to a vigorously stirring solution of 2-iodo-1,3-diisopropylbenzene (691 mg, 2.4 mmol) in 6 ml of diethyl ether. The mixture was stirred additionally for 15 min at -60 °C, warmed up to room temperature and stirred for another 1h. Then the solution was cooled to -90°C, and $BF_3{\cdot}OEt_2$ (0.15 ml, 170 mg, 1.2 mmol) was added via syringe in one portion. The mixture was allowed to warm to room temperature and stirred overnight. The solvent was removed under reduced pressure; the residue was suspended in 10 ml of toluene and filtered. The filter cake was washed with additional portions of toluene (5x1 ml), and the filtrate was evaporated to dryness yielding 403 mg bis(2,6-diisopropylphenyl) fluoroborane ($Dipp_2BF$): as slightly yellow oil (95.4%), which was used without further purification. ^{1}H NMR (500 MHz, CD_2Cl_2, 25°C): δ 7.21 (m, 2H), 7.05 (m, 4H), 3.17 (m, 4H), 1.13 (d, J_{HH} =6.7 Hz, 24H). ^{19}F NMR (282 MHz, C_6D_6): δ -178.27 (s). Obtained as described above, Mes_2BF was redissolved in 6 ml of toluene and the solution was cooled to -70°C. The solution of [2-(2,2,6,6-tetramethylpiperidin-1-yl)phenyl]lithium (**66**) (270 mg, 1.2 mmol) in 4 ml of toluene was added via syringe in one portion. The mixture was allowed to warm to room temperature and heated in an oil bath at 60°C overnight. The solvent was removed under reduce pressure; the residue was suspended in 10 ml of toluene and filtered. The filter cake was washed with additional portions (5x1 ml) of toluene and the filtrate was evaporated to dryness yielding 0.610mg (>90%) of crude yellow oil containg *ansa*-aminoborane **69-Dipp** as major compound and residual amount of unreacted Mes_2BF. ^{1}H NMR (500 MHz, C_6D_6): δ 7.54 (dd, J_{HH} = 7.6, 1.9 Hz, 1H), 7.34 (t, J_{HH} = 7.8 Hz, 1H), 7.27 (m, 1H), 7.23-7.18 (m, 3H), 7.11-7.06 (m, 2H), 7.04-6.98 (m, 2H), 3.88 (hept, J_{HH} = 6.8 Hz, 2H), 3.42 (hept, J_{HH} = 6.2 Hz, 2H), 3.02 (hept, J_{HH} = 7.3, 6.6 Hz, 2H), 2.49 (hept, J_{HH} = 6.8 Hz, 2H), 1.58-1.44 (m, 12H), 1.37-1.31 (m, 4H), 1.25 (d, J_{HH} = 6.8 Hz, 3H), 1.23-1.06 (m, 8H overlapped with protons of residual starting material), 0.98 (d, J_{HH} = 6.5 Hz, 3H), 0.83 (s, 3H), 0.77 (m, 6H), 0.69 (s, 3H), 0.62 (d, J_{HH} = 6.4 Hz, 3H), 0.58 (d, J_{HH} = 6.6 Hz, 3H).

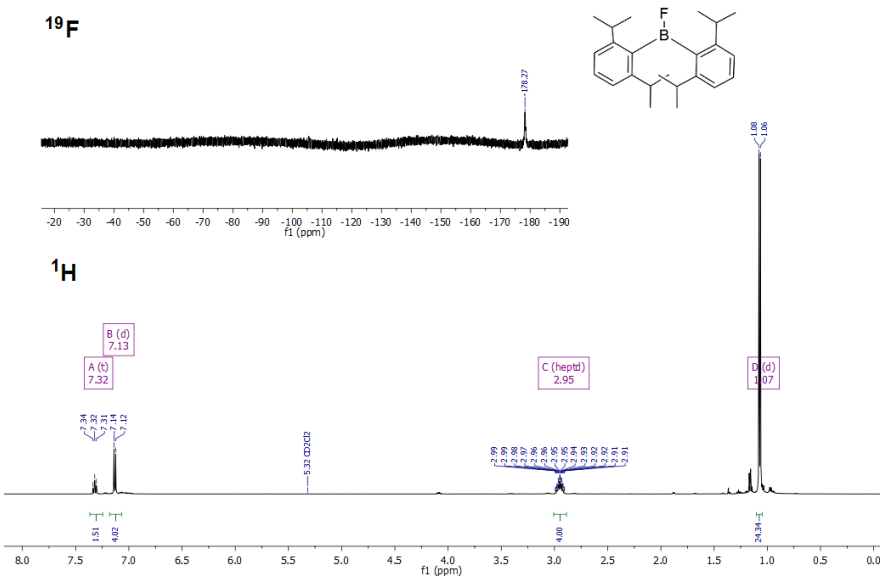

Figure 37 ^{1}H NMR (300 MHz, C_6D_6, 25°C) and 19F (282 MHz, C_6D_6, 25°C) spectra of compound Mes_2BF, precursor of **69-Dipp.**

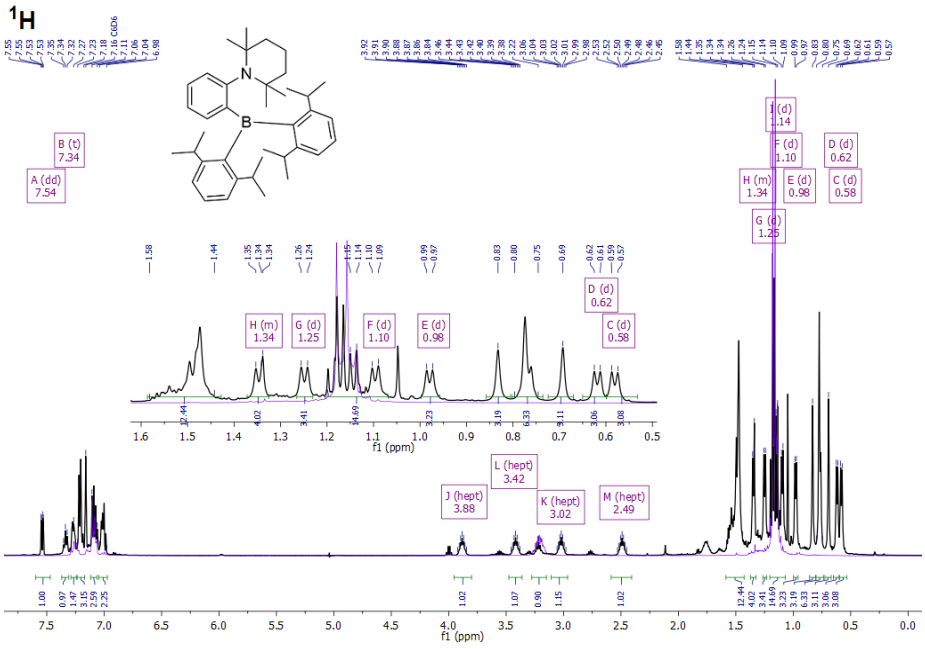

Figure 38 ^{1}H NMR (300 MHz, C_6D_6, 25°C) spectrum of compound of crude **69-Dipp.**